

University of Montana

ScholarWorks at University of Montana

Graduate Student Theses, Dissertations, &
Professional Papers

Graduate School

2004

On the nature of volcanic lithic fragments: Definition source and evolution

Matthew Dale Affolter
The University of Montana

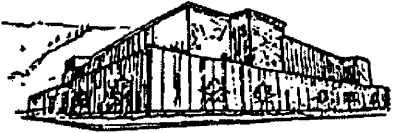
Follow this and additional works at: <https://scholarworks.umt.edu/etd>

Let us know how access to this document benefits you.

Recommended Citation

Affolter, Matthew Dale, "On the nature of volcanic lithic fragments: Definition source and evolution" (2004). *Graduate Student Theses, Dissertations, & Professional Papers*. 7561.
<https://scholarworks.umt.edu/etd/7561>

This Thesis is brought to you for free and open access by the Graduate School at ScholarWorks at University of Montana. It has been accepted for inclusion in Graduate Student Theses, Dissertations, & Professional Papers by an authorized administrator of ScholarWorks at University of Montana. For more information, please contact scholarworks@mso.umt.edu.



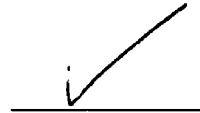
**Maureen and Mike
MANSFIELD LIBRARY**

The University of
Montana

Permission is granted by the author to reproduce this material in its entirety, provided that this material is used for scholarly purposes and is properly cited in published works and reports.

****Please check "Yes" or "No" and provide signature****

Yes, I grant permission



No, I do not grant permission



Author's Signature: _____

Date: _____

5-12-4

Any copying for commercial purposes or financial gain may be undertaken only with the author's explicit consent.

**ON THE NATURE OF VOLCANIC LITHIC FRAGMENTS:
DEFINITION, SOURCE, AND EVOLUTION**

by

Matthew Dale Affolter

B. S., University of California, Los Angeles, 2002

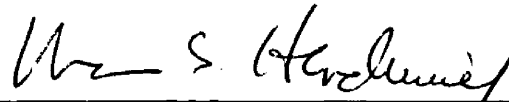
Presented in partial fulfillment of the
requirements for the degree of

Master of Science

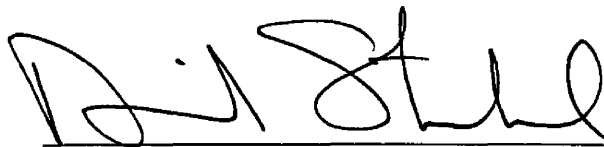
THE UNIVERSITY OF MONTANA

2004

Approved by:



Advisor



Dean, Graduate School

5-12-04

Date

UMI Number: EP38362

All rights reserved

INFORMATION TO ALL USERS

The quality of this reproduction is dependent upon the quality of the copy submitted.

In the unlikely event that the author did not send a complete manuscript and there are missing pages, these will be noted. Also, if material had to be removed, a note will indicate the deletion.



UMI EP38362

Published by ProQuest LLC (2013). Copyright in the Dissertation held by the Author.

Microform Edition © ProQuest LLC.

All rights reserved. This work is protected against unauthorized copying under Title 17, United States Code



ProQuest LLC.
789 East Eisenhower Parkway
P.O. Box 1346
Ann Arbor, MI 48106 - 1346

ACKNOWLEDGMENTS

First of all, I would like to let the reader know that I really wanted this project to work. If successful, the application of this technique would be almost unfathomable, and could carry my research career for years to come. No one wanted it to work more than me. So to Ray, Bill, and all the rest, sorry, maybe next time.

This project was primarily funded by the University of Montana McDonough Scholarship. Special thanks to the donors: Mrs. Jean McDonough, Mr. Cortland S. Dietler, Mr. Donald E. Hockaday, Jr., Mr. Victor Stabio, Mr. Joseph Kimmitt, Mr. Chesley Pruet, and Mr. Richard Cox. Let it be known that every successful step in my life will be only a step closer to the goal of mine: establishing a legacy not only for future McDonough scholars, but for other programs with similar goals of supporting young scientists. Thanks to Marc Hendrix for helping me with the McDonough Scholarship process and the faculty of the University of Montana for approving my project.

The idea of this project was from Ray Ingersoll, my old sed professor at UCLA. He always wanted someone to work out the relationships between volcanic lithic fragments and parent volcanic rock. When I was having trouble finding a project to do here at UM, I asked Ray if I could do his project, and he agreed, and has added much to the project and my personal knowledge in general. By the way, I promise I will finish my undergrad thesis soon, Ray. Marc Hendrix, my advisor, was slightly skeptical about the thesis idea at first, mainly due to funding issues. I eventually talked him into it. Throughout the entire thesis process, Marc has been completely supportive and helpful. His only fallback is that too many people know how helpful he is, so it's hard to steal him away from the rest of the department. Don Winston and Rudy Gideon were also great as my other thesis advisors, when they could understand what I was saying. I tend to not make a lot of sense. The rest of my technical support team includes, but is not limited to: W. R. Dickinson, Kathie Marsaglia, Bill Heins, Gary Smith, Bob Wintsch, Carol Dehler, Linda Kah, Don Hyndman, Nancy Hinman, Charlie Bacon, Nancy Riggs, Gray Thompson, Michael Hofmann, Michael Sperazza, Erik Katvala, Ryan Portner, and Jeremy Boyce.

The number of people I need to thank is ridiculous, but I'm gonna try. First, special thanks to Todd Feeley, Jon Davidson, Bob Christiansen, and John Hora for providing samples. Thanks to Ram Alkaly for doing thin sections for me at the UCLA student rate. Happy retirement, Ram. Thanks to the entire UM Geology program, including: Rachele Ambrose, Amy Bondurant, Liza Briggs, Erik Burtis, Andrew "Thug" Caruthers, Brian Collins, Robyn Cook, Aaron Deskins, Cain Diehl, Michelle Foster, Emily Geraghty, Emily Godfrey, Nathan Harrison, Chris Hawkins, Matt Hertz, Danielle Hughes, Adam Johnson, Susan Joy, Rebecca Kunz, Nick Laatsch, Kevin Loustaunau, Layaka Spring Rainbow Mann, Rachel McCool (thank you most of all), John "Sweet Pickles" Mocko, fellow Bruin Prof. Johnie Moore, Beau Palister, Sheetal "Beetle" Patel, Noel Philip, Ryan "The Hebrew Hammer" Portner, Damien Powledge, Prof. Jim Sears,

Prof. Steve Sheriff, Prof. Derek Sjostrom, Jeremy Stalker, Ben Swanson, Garrett Timmerman, Matt Vitale, Prof. Bill Woessner, and Matt Zunker. Extra special thanks to Christine Foster and Loreene Skeel, who keep all of us functioning.

Thanks also to the UCLA Geology crew - Chris Avalos (a.k.a. Dueñas), Prof. Gary Axen, Prof. Peter Bird, Jessica Block, Mason Chuang, Roopl Chauhan, Kari Cooper, Prof. Wayne Dollase, John Duhl, Kristin Ebert, Hannah Gabriel, Bernard Guest, Lauri Holbrook, Mary Kairouz, Pat Lam, Teresa Lassak, Lorraine Leon, Prof. Craig Manning, M. Alex Matiella, Eric Middelstaedt, Sheila Morrissey (who just LOVES Missoula), Brian Murray, Andy Nguyen, Alex Robinson, Kelly Shiozaki, Josh Sussman, Joy Szmanski, Mike Taylor, Masataka Tsunetani, Jorge Vasquez, Prof. John Vidale, Madeline Wright, Nadia Yglecias, Prof. An Yin, and Jennifer Zamora.

Personal thanks to: Mom and Dad, Daryl, Grandma Jo, the Raffel-Smith Family, Alicia Raffel, the Robles Family, Armando Franco, Fernando Chavez, Gabriel Serrano and all of 520 Kelton #407, Esteban Galvan, Angie Lewis, Debbie Steinert, Ed Victoria, Ken Barker, Sally Rodrick, Steve Joiner, Jackie Cohen, SJSU chapter of Gamma Zeta Alpha, M. Scioscia and the boys, B. Howland and the boys. No thanks to: everyone at 'sc, past, present, and future (except Lorraine), and everyone who would not help me and discourage me along the way (you know who you are). Future thanks to Cari Johnson and everyone at U of U. It's gonna be great!

A final thanks goes to you, the reader, who ever you are. I'm impressed if you made it all the way through this silly section without skipping ahead. Anyway, please enjoy, and if you find any of this to be inappropriate or offensive, just remember, it's only a thesis.

LIST OF TABLES

1. Volcanic lithic definitions	4
2. Point counting criteria	24
3. Replication data and statistics	29
4. Sample database	32
5. Analysis of first order data	50
App 1. Complete point count dataset	58

INTRODUCTION

In his landmark 1970 study, *Interpreting Detrital Modes of Graywacke and Arkose*, William R. Dickinson established the modern methods of classifying the composition of sandstones. Dickinson (1970) classified volcanic rock fragments into four categories: felsitic, microlitic, lathwork, and vitric (Figure 1). These categories are based upon common volcanic rock textures, and each category was assigned to a general composition of derivation: felsitic texture to silicic volcanic rocks, microlitic texture to intermediate compositions, and lathwork texture to basaltic compositions. Vitric texture corresponds to glass-rich volcanics, which are most common in high silica rhyolites.

Since Dickinson's (1970) paper, sandstone petrology has advanced greatly. Despite this, relationships between the composition of the source volcanic rock and the texture of the volcanic rock fragments (now referred to as volcanic lithic fragments) type have not been demonstrated. My goal in this study is to establish the true statistical relationship between volcanic lithic fragments and specific parent volcanic rock composition, so that the technique can be tested and, if needed, refined. This work could have important applications in all provenance studies in which volcanic lithic fragments are used to infer information regarding volcanic rocks in source areas.

One aspect of volcanic lithic fragments that has never been clearly defined is the placement of boundaries between the different categories. Even Ingersoll and Cavazza (1991), which provided a more detailed definition of volcanic lithic fragments, several of the boundaries are stated as "gradational," without further explanation. I contend that by examining crystal textures closely, volcanic lithic fragment categories become more straightforward and definable. Below I propose a revised set of lithic categories with

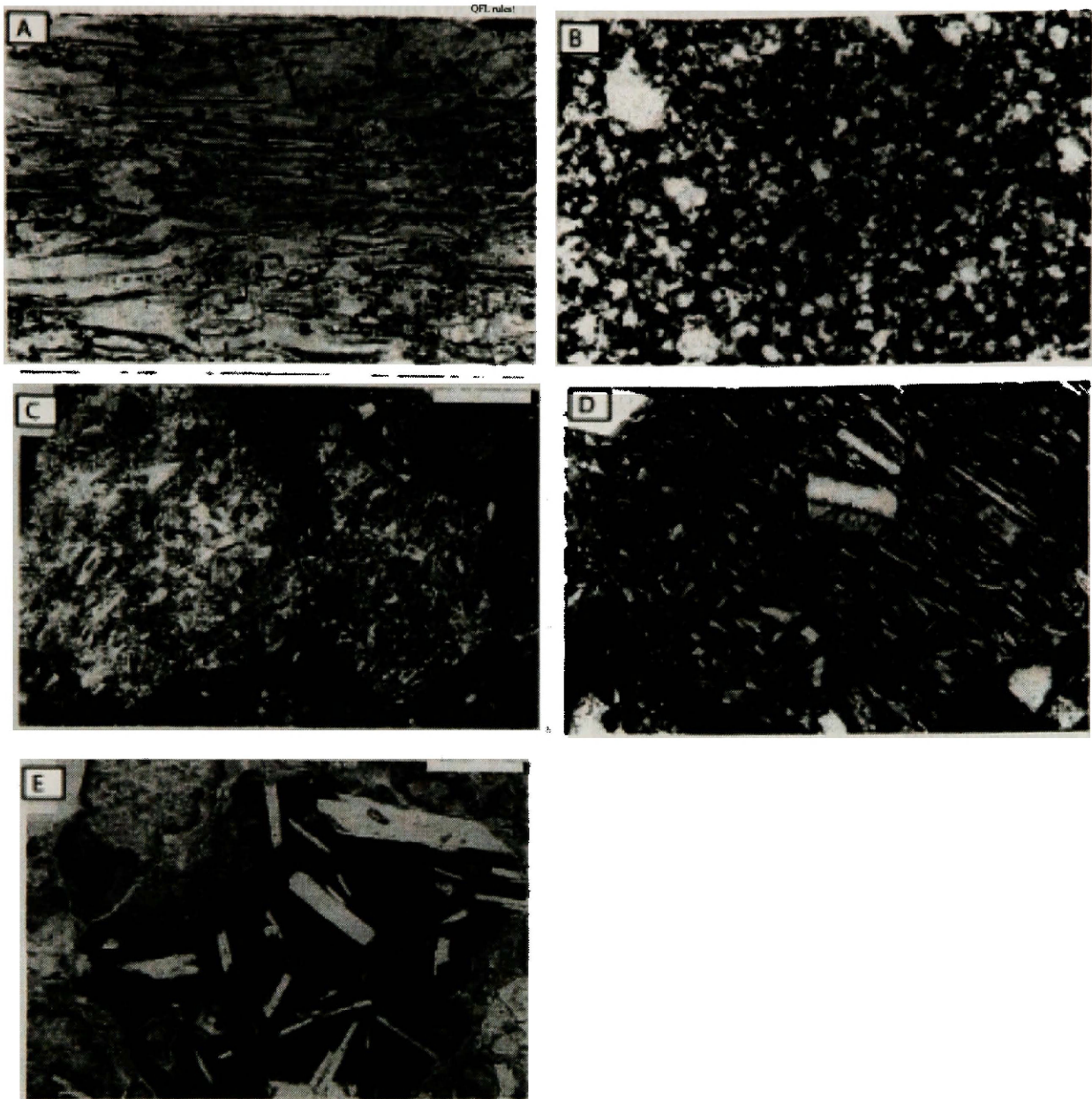


Figure 1. Photomicrographs of the classic volcanic lithic fragments of Dickinson (1970).

(A) Vitric grain showing flow patterns, plane-polarized light. (B) Felsitic (granular) grain showing chert-like appearance, crossed-polarized light. (C) Felsitic (seriate) grains, with an irregular mosaic of crystals, crossed-polarized light. (D) Microlitic grain, with dominant plagioclase feldspar microlites, crossed-polarized light. (E) Lathwork grain, with large plagioclase feldspar laths, crossed-polarized light. Picture width is 0.5 mm in (A), (B), and (D), scale bar is 0.2 mm in (C) and (E). (A), (B), and (D) from Ingersoll and Cavazza (1991), (C) and (E) from Critelli and Ingersoll (1995).

particular attention paid to defining the boundaries between categories (Table 1).

An intrinsic but not explicit part of Dickinson's (1970) classification is the relative percentage of microlites (birefringent, microscopic volcanic minerals) and glass in the matrix (non-phenocryst phase) of each lithic type. Vitric lithic fragments have nearly no microlites and all glass, felsitic lithic fragments have all microlites and almost no glass, microlitic lithic fragments have approximately equal amounts of microlites and glass, and lathwork lithic fragments have high glass, low microlites, and large phenocrysts. My classification system takes this relationship between microlites and glass into account as a determining factor between the lithic fragment types.

This project primarily deals with zero order samples (Ingersoll, 1990), which are unaltered, unweathered, volcanic rocks in their original state. I chose volcanic rocks in which the whole-rock geochemistry is known. In order to have a better understanding of the effects of transport on volcanic lithic fragments in real world settings, I examined downslope trends of first order samples (Ingersoll, 1990) with an emphasis on degradation factors, mainly, the amount of glass in the volcanic lithic fragment population.

Previous Work

Many papers have used the definitions of volcanic lithic fragments presented in Dickinson (1970) and Ingersoll and Cavazza (1991). Most applications focus on the relationship of sandstone composition, provenance, and tectonic setting (Dickinson and Suczek, 1979). Graham et al. (1976) used volcanic lithic fragments to link collision sequences. Ingersoll and Cavazza (1991) and Large and Ingersoll (1995) used detailed descriptions of the volcanic lithic fragments to better understand volcanic dispersal patterns and tectonics in New Mexico. Horton et al. (2002) and Carroll et al. (1995)

Table 1

Volcanic Lithic Definitions, past and present

Lv type	Dickinson (1970)	Ingersoll & Cavazza (1991)	This study
Vitric	... glass or altered glass, which may be phyllosilicates, zeolites, feldspars, silica minerals, or combinations of these in microcrystalline aggregates.	... glass or altered glass, which may be phyllosilicates, zeolites, feldspars, silica minerals, or combinations of these in microcrystalline aggregates.	95-100% glass, 0-5% anhedral, subhedral, and euhedral microlites in the matrix.
Felsitic	... anhedral, microcrystalline mosaic, either granular or seriate, composed mainly of quartz and feldspar ...	Granular: ... anhedral microcrystalline mosaics, with uniform very fine grain size, composed mainly of quartz and feldspar ... devitrified-vitric grains are gradational with granular ... Seriate: ... anisometric mosaics, with wide ranges of grain sizes and shapes, composed mainly of quartz and feldspar ...	Granular: 5-100% anhedral microlites, 0-95% glass, 0-5% subhedral and euhedral microlites in the matrix. Seriate: 0-5% glass, 5-100% subhedral microlites, 0-95% anhedral microlites, 0-50% euhedral microlites in the matrix.
Microlitic	... subhedral to euhedral feldspar plates and prisms in pilotaxitic, felted, trachytic, or hyalopilitic patterns of microlites subhedral to euhedral feldspar plates and prisms (less than 0.0625 mm in maximum dimension) in pilotaxitic, felted, trachytic, or hyalopilitic patterns of microlites ...	25-50% glass, 50-75% subhedral to euhedral microlites in the matrix.
Lathwork	... plagioclase laths in intergranular and intersertal textures plagioclase laths in intergranular and intersertal textures... this category is gradational with microlitic.	50-95% glass, 5-50% subhedral to euhedral microlites in the matrix.

reported similar studies in the Andes and in northern China, respectively. Lundberg (1991), Marsaglia (1992), and Marsaglia and Ingersoll (1992) used volcanic lithic type to differentiate sands from different tectonic settings. Marsaglia (1993) used the volcanic lithic fragment textures and glass color to characterize the sediment composition of the Hawaiian Islands. For a discussion on paleovolcanic vs. neovolcanic (noncoeval vs. coeval) lithic fragments, see Critelli and Ingersoll (1995).

METHODS

Matrix Crystalline Textural Types

The following four primary matrix crystalline textural types characterize most, if not all, volcanic rocks when viewed with a petrographic microscope. Most volcanic rocks contain large crystal phenocrysts and glassy and/or microlites (birefringent, microscopic, volcanic minerals) in the matrix. These crystalline textural types are based upon the types of microlites and their relative proportion to glass within the matrix. These criteria are similar to descriptions of volcanic materials in Williams et al. (1954).

Phenocryst crystals are not used in this study for many reasons. Firstly, the abundance or presence of phenocrysts does not depend on to composition. Secondly, volcanic lithic fragments can only have a volcanic source, whereas common volcanic minerals can occur in a wide variety of rocks other than volcanics. Thirdly, phenocrysts can yield information regarding the volcanic history independent of the matrix, and have been extensively studied by previous authors (e.g., Nesse, 1991). However, matrix in volcanic rocks has not been studied in detail with regard to composition. Most importantly, aphanitic lavas (lavas without phenocrysts) would disrupt a system based upon, or even partially based upon, phenocrysts.

The primary goal of these matrix crystalline textural types is to have a classification scheme based solely on the descriptive attributes of crystal form and style applicable to volcanic lithic fragments, rather than specific igneous textures or mineralogy, so the assignment of lithic fragment type is more inclusive.

Glass

The first of the major matrix types is volcanic glass (Figure 2). Volcanic glass is volcanic matrix that is non-crystalline, transparent, and isotropic, and is common in pumice, ash, and obsidian. Glass in framework grains is normally altered to clays, oxides, and silicates in the sedimentary environment, obscuring its identification. Alteration of glass can give it varied amounts of birefringence and a pseudo-crystalline appearance. When possible, these alteration effects are ignored and the area in question is noted as glass. Vesiculation, flow patterns, and aligned phenocryst phase minerals can aid in the identification of glass. Highly altered glass, volcanic chert, and other alteration byproducts are not used in this study.

Anhedral

The second matrix crystalline textural type is *anhedral* (Figure 3). These are microlites that show a crystalline habit, especially when examined under crossed polars, but the crystal faces are not defined. Most crystal faces in anhedral microlites seem to overlap, almost like extinction in a grain of chert. This is due to the fact that anhedral crystals are smaller in diameter than the thickness of the slide (30 μm), and thus, microlite margins overlap each other over the thickness of the thin section. The crystals have little recognizable form, as individual crystals are mainly equant and of a similar relative size.

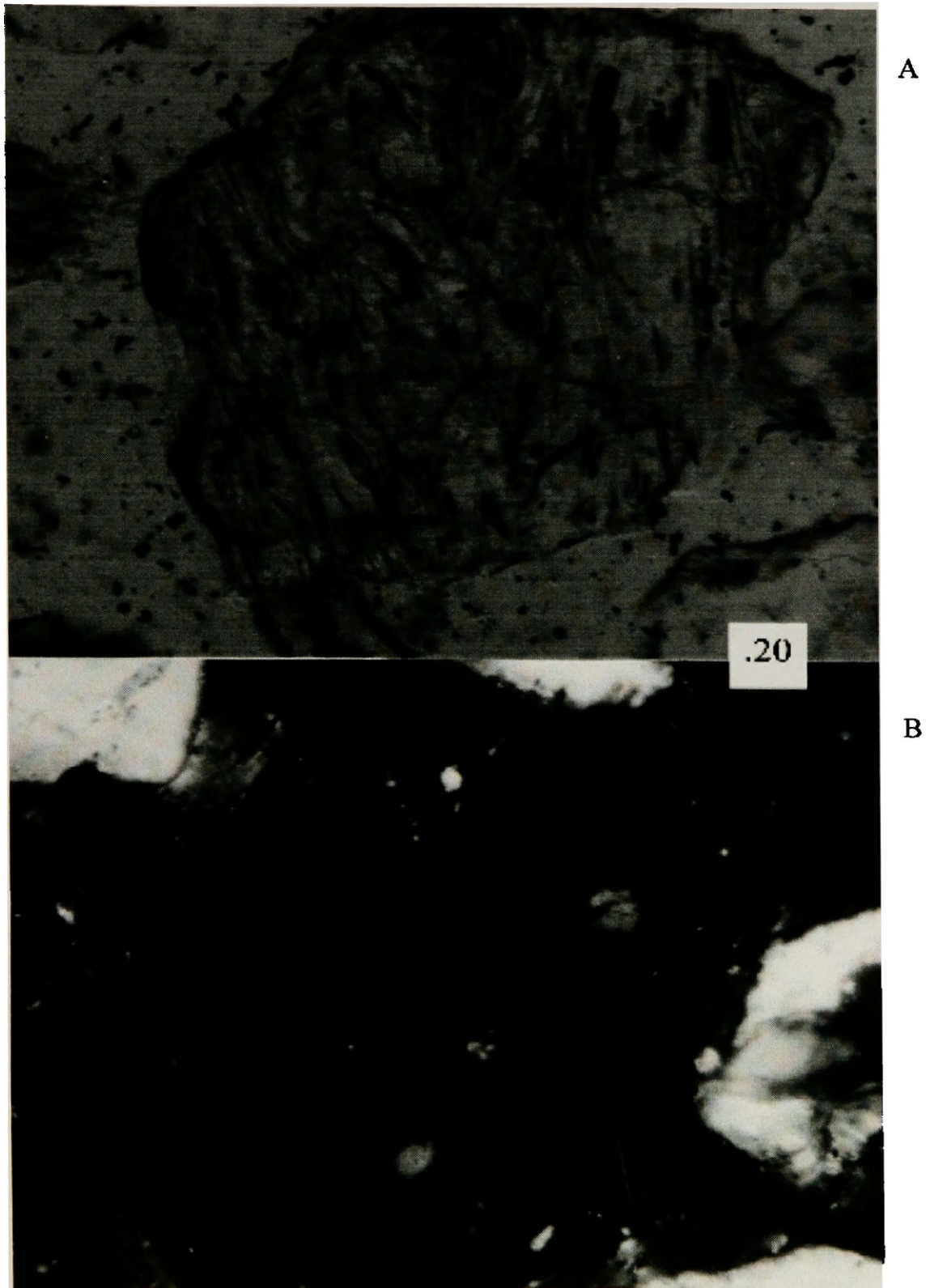


Figure 2. Vitric lithic fragment made of almost 100% glass. Note vertical flow pattern. Modern sand from the Owens River Gorge, derived from the .76 Ma Bishop Tuff. Sample BT 1A-c, 50X magnification, plane polarized light, (ppl, A) and cross polarized light (xpl, B). Square is 0.20 mm across.

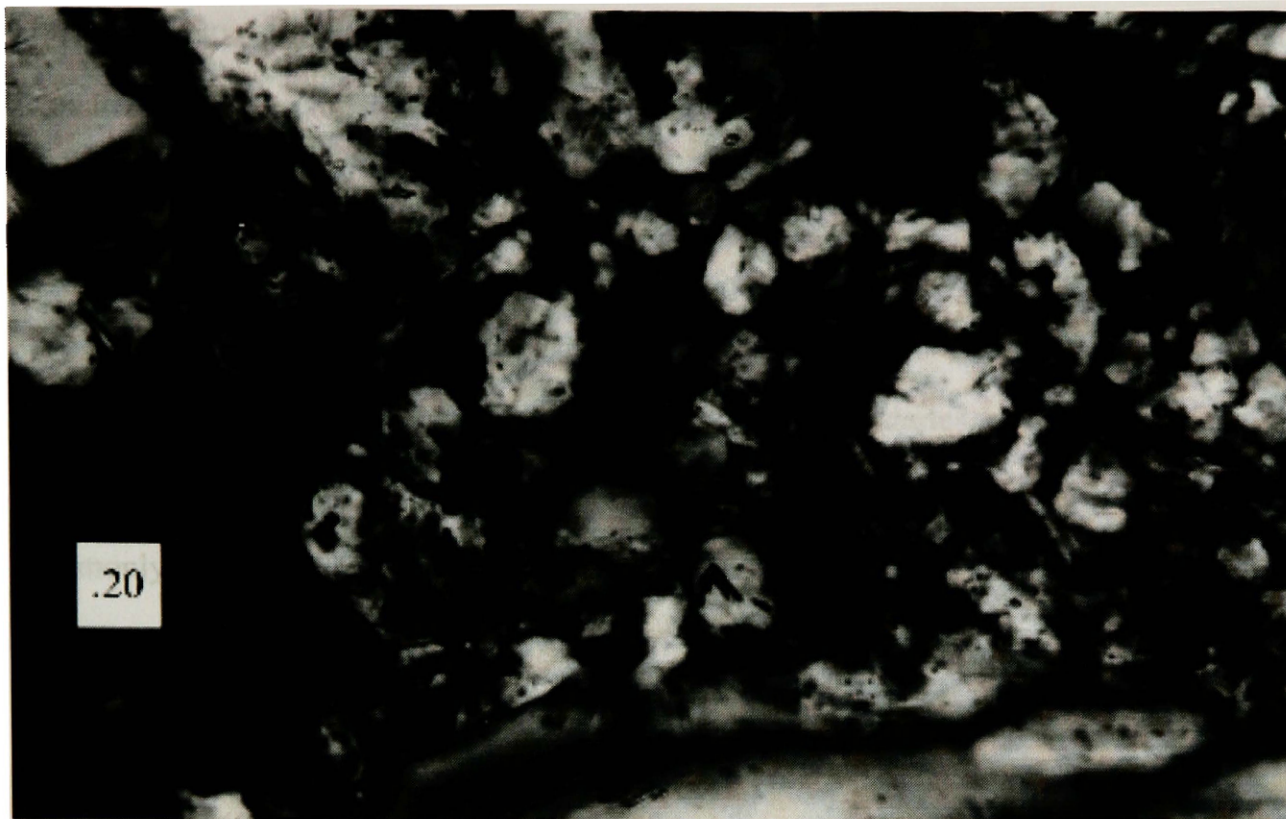


Figure 3. Anhedral microlites, showing equant microlites and no clear crystal faces or forms. Holocene andesite from Martinique, Lesser Antilles. M8228, 125X, xpl. Square is 0.20 mm across.

The mineralogy of these microlites can vary but is commonly made of felsic minerals such as quartz and feldspar (Dickinson, 1970; Ingersoll and Cavazza, 1991).

Subhedral

The third category of matrix crystalline texture is *subhedral* (Figure 4). Subhedral grains are microlites that have one or more well defined boundaries, or several moderately defined boundaries. With subhedral microlites, the form of the mineral in question is commonly recognizable, if not diagnostic of a specific mineral. Each microlite is distinct in crossed-polarized light, but the boundaries may be somewhat vague.

Euhedral

The fourth and final matrix crystalline textural type is *euhedral* (Figure 5). This includes microlites that have well defined boundaries and forms.

Application to Existing Volcanic Lithic Fragment Categories

Based upon the above parameters, I propose the following refinement of the volcanic lithic fragment categories. Use of these matrix crystalline textural categories provides a solid basis for the identification of volcanic lithic fragments. When examining a grain, I simply ascertain the relative proportions of the matrix types and use them to define volcanic lithic fragment categories. I redefined each lithic fragment category (Ingersoll and Cavazza, 1991; Dickinson, 1970), with a specific and clear range of each type of matrix category (Figure 6). My main goal in redefining volcanic lithic fragment boundaries was to make the system user friendly by using easily manageable percentages in the detection system (5%, 25%, 50%).

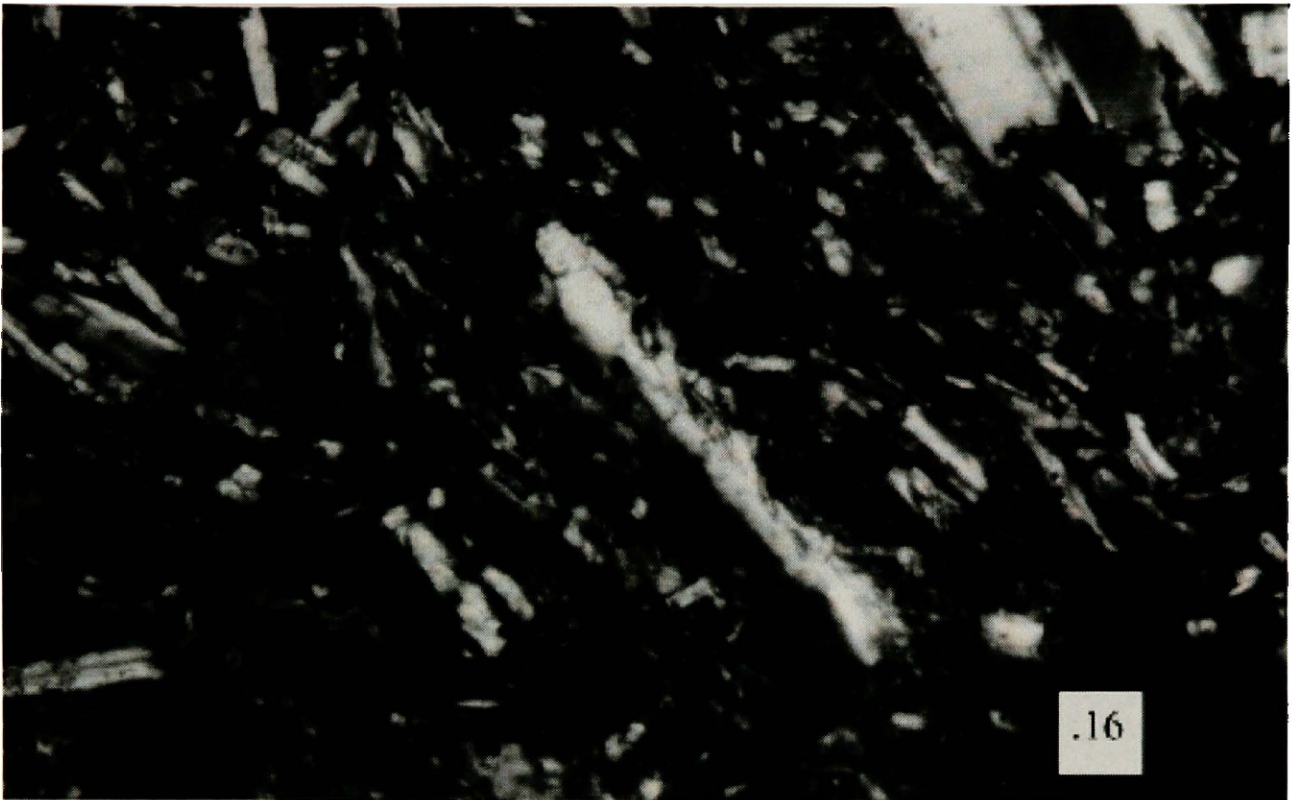


Figure 4. Subhedral microlites, showing partial and/or poorly developed crystal faces. Picture taken of a Holocene basalt from Martinique, Lesser Antilles. M8328, 63X, xpl. Square is 0.16 mm across.

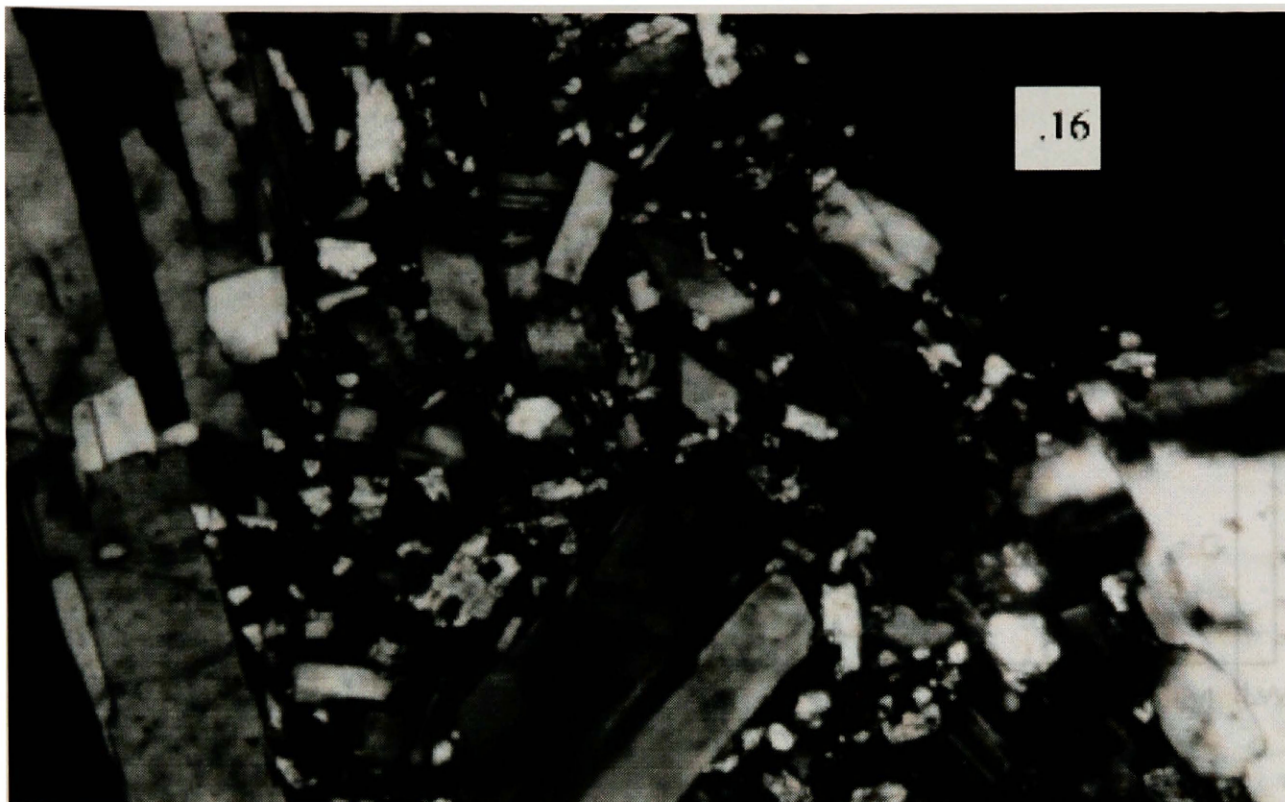


Figure 5. Euhedral microlites, showing complete and/or well developed crystal faces. From a Holocene basalt on Redonda, Lesser Antilles. R8204, 63X, xpl. Square is 0.16 mm across.

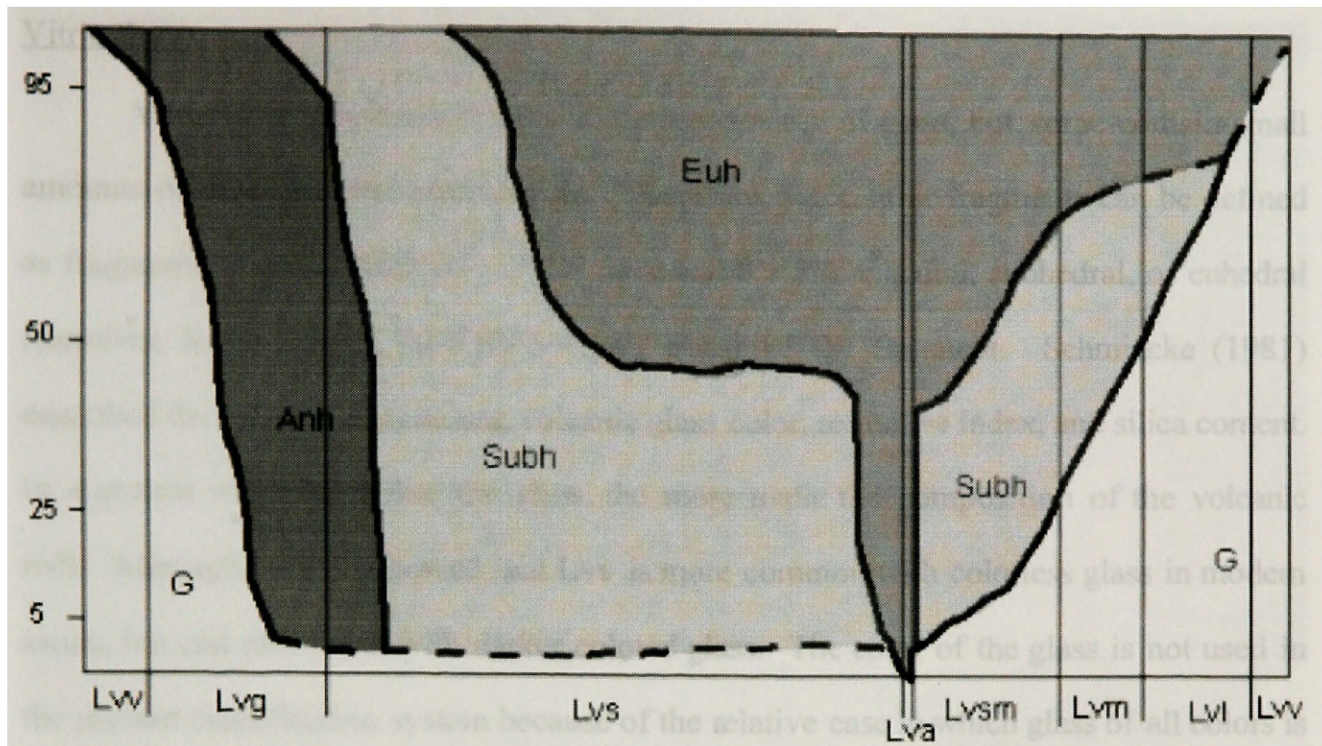


Figure 6. Schematic diagram showing volcanic matrix crystalline textural type and their relative proportions with respect to the new volcanic lithic fragment definitions proposed in this study. Inferred increasing silica content toward left, based upon Ingersoll and Cavazza (1991) and Dickinson (1970). Curves and areas are strictly schematic. Dashed lines indicate approximate and/or unknown behavior of the matrix types. Note the lower glass content for ‘intermediate’ composition lithic fragment populations and higher glass content for ‘high’ and ‘low’ silica composition lithic fragment populations. G=glass, Anh=anhedral, subh=subhedral, euh=euhedral, Lvv=vitric lithic fragment, Lvg=granular lithic fragment, Lvs=seriate lithic fragment, Lva=aggregate lithic fragment, Lvsm=submicrolitic lithic fragment, Lvm=microlitic lithic fragment, Lvl=lathwork lithic fragment.

Vitric (LvV)

Vitric lithic fragments (Figure 2) consist mainly of glass, but some contain small amounts of microlites and phenocrysts. Therefore, vitric lithic fragments can be defined as fragments which contain 95 - 100% glass and 0 - 5% anhedral, subhedral, or euhedral microlites in the matrix (non-phenocryst) phase of the fragment. Schmincke (1981) described the relationships among volcanic glass color, refractive index, and silica content. In a general way, the darker the glass, the more mafic the composition of the volcanic rock. Marsaglia (1992) showed that LvV is more common with colorless glass in modern sands, but can also occur with darker colored glass. The color of the glass is not used in the present classification system because of the relative ease in which glass of all colors is altered to oxides, clays, and other minerals in the sedimentary environment (Figure 7).

Granular (Lvg)

Granular lithic fragments (Figure 8) contain mostly anhedral microlites in the matrix, but some contain glass and limited subhedral microlites in the matrix. They are defined as consisting of 5 - 100% anhedral microlites, 0 - 95% glass, and 0 - 5% subhedral to euhedral microlites in the matrix. Note that it is very uncommon to find volcanic rocks or lithic fragments that have subequal amounts of both anhedral microlites and glass. In my experience, most samples are rocks rich in glass or anhedral microlites.

Seriate (Lvs)

Seriate lithic fragments (Figure 9) are known for the wide range of crystal forms, sizes, and types. Seriate lithic fragments contain 0 - 5 % glass, 5 - 100% subhedral microlites, 0 - 95% anhedral microlites, and 0 - 50% euhedral microlites in the matrix.

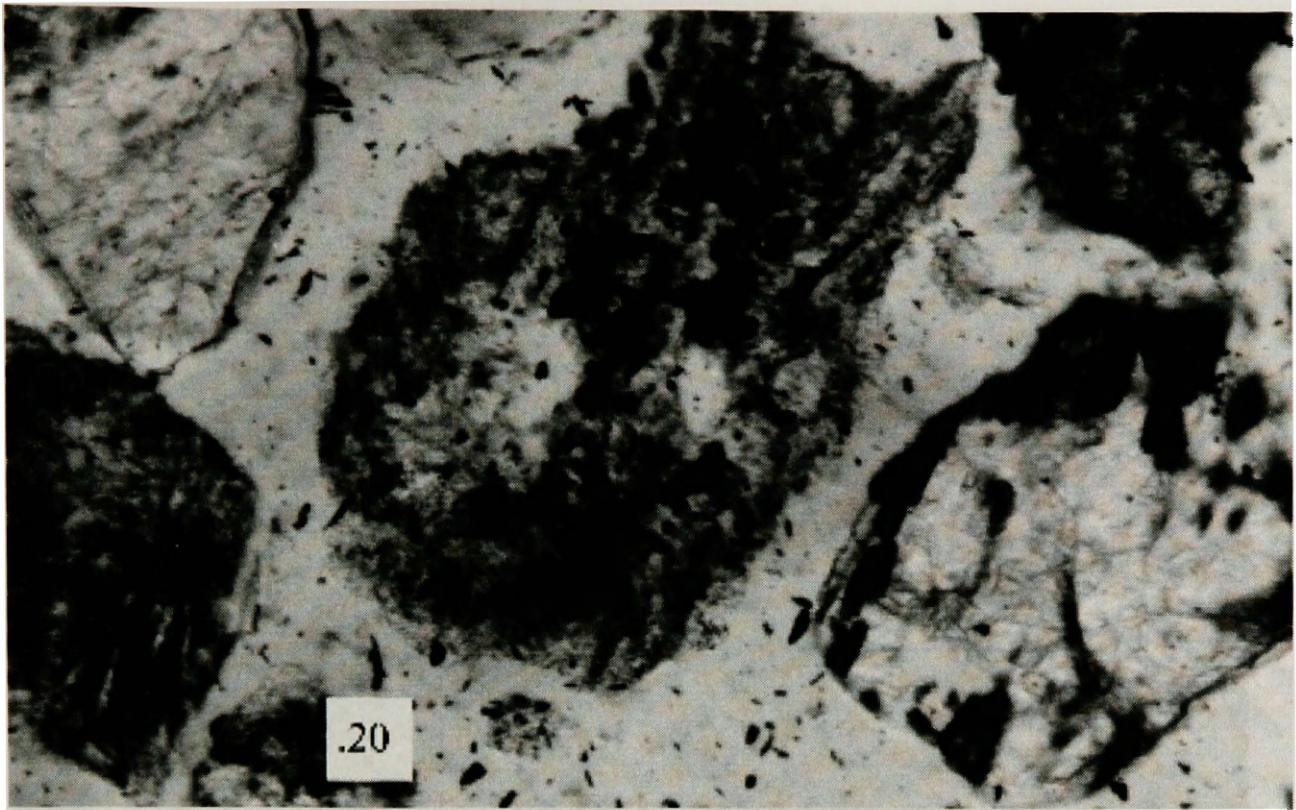


Figure 7. An example of the variety of colors of glass produced from the same lava, in this case, the Bishop Tuff. The differences in color are most likely due to differences in weathering of each grain. All of these grains would be counted as Lv. BT 1B-f, 50X, ppl. Square is 0.20 mm across.

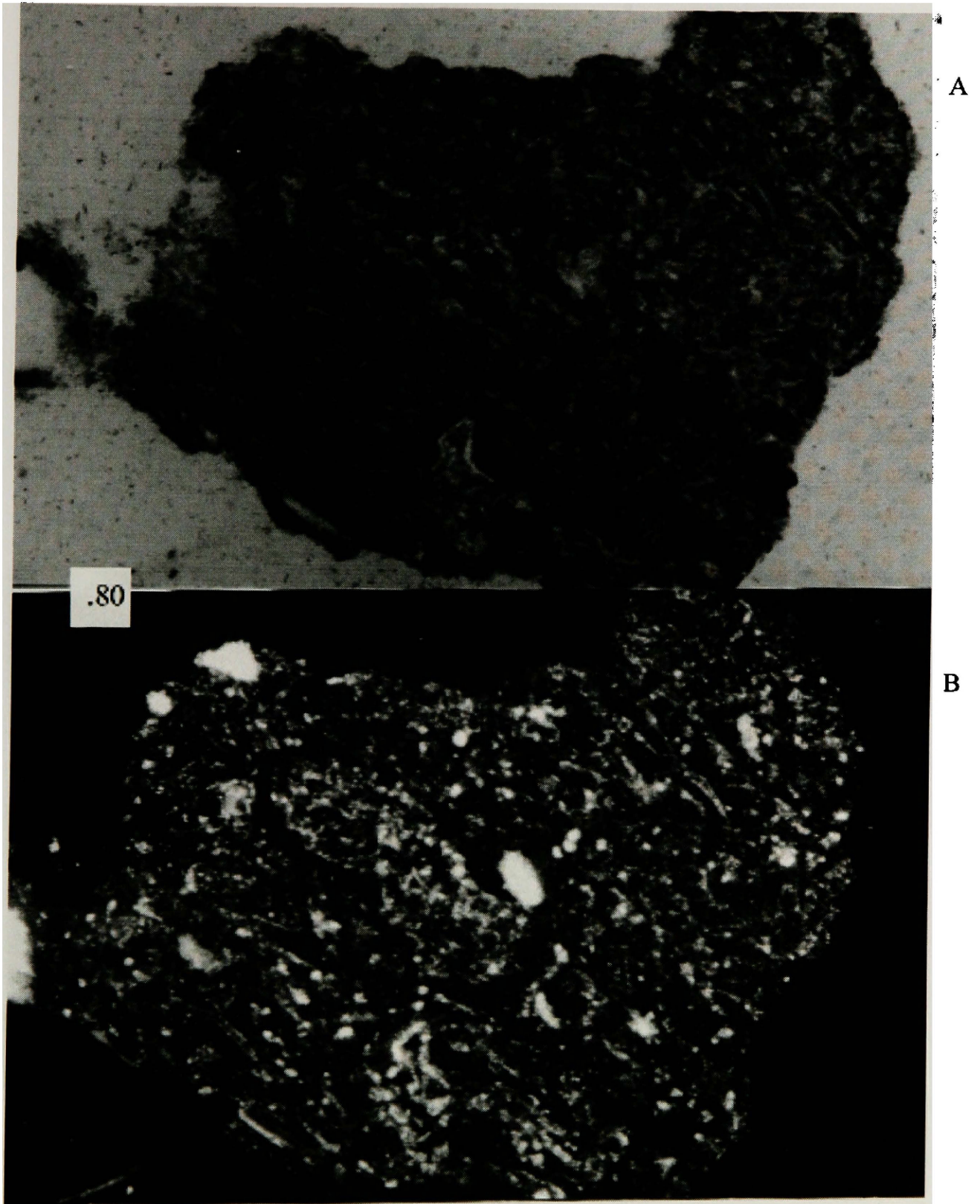


Figure 8. Granular lithic fragment, made of approximately 90% anhedral microlites and 10% glass. From modern sand of the Bishop Tuff. BT 1A-c, 12.5X, ppl (A) and xpl (B). Square is 0.80 mm across.

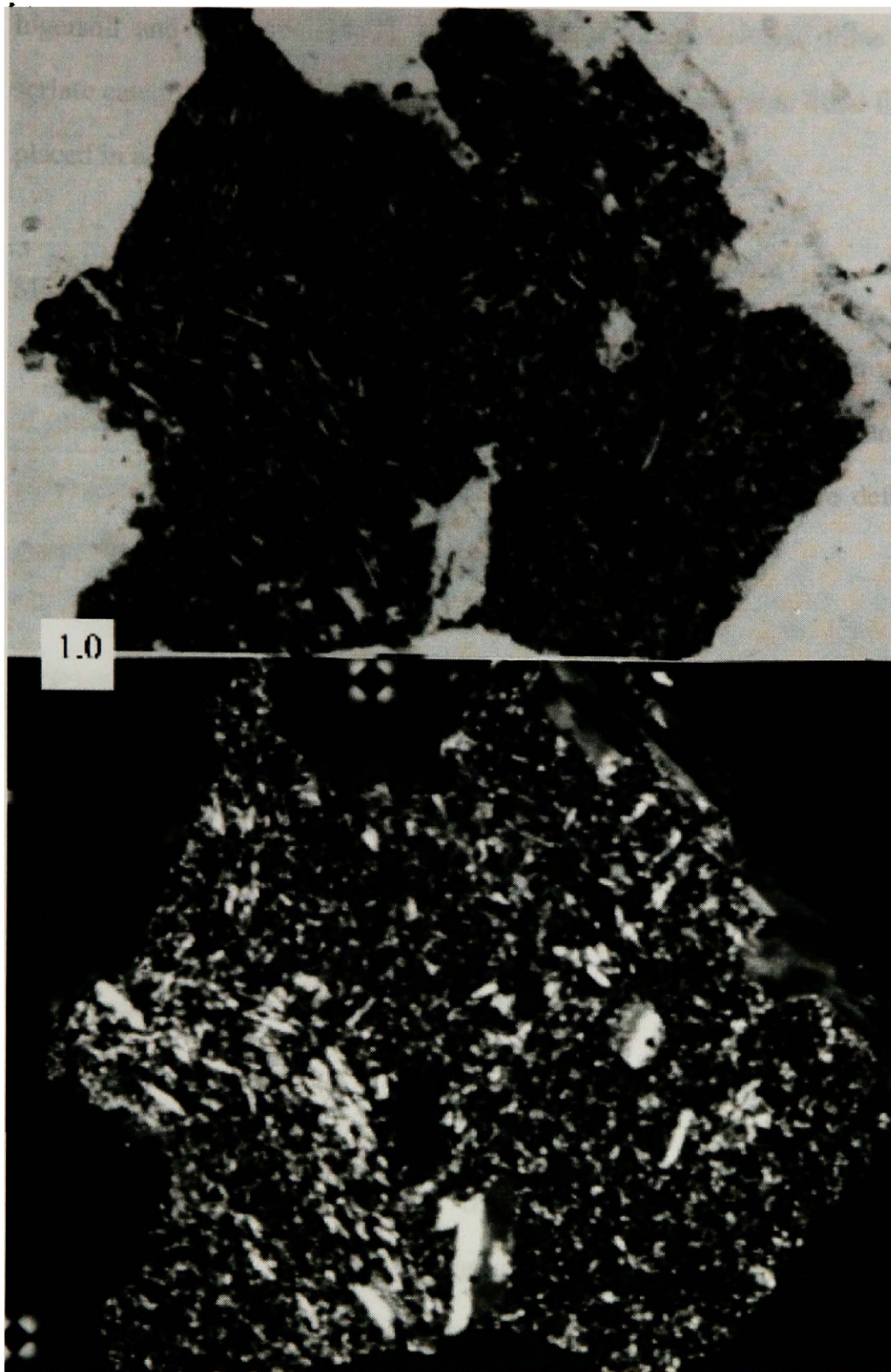


Figure 9. Seriate lithic fragment, made of 100% subhedral and euhedral microlites. From modern sand of the Red Hill cinder cone. COS 1B-c, 10X, ppl (A) and xpl (B). Dark microlites in top are various oxide minerals. Phenocryst in bottom center is plagioclase feldspar. Square is 1.0 mm across.

Ingersoll and Cavazza (1991) included undetermined volcanic lithic fragments in the seriate category. In this study, however, undetermined volcanic lithic fragments would be placed in a category called Lvu (see below).

Microlitic (Lvm)

Volcanic lithic types, like microlitic and lathwork, have an important component of glass, but the glass in these lithic fragments are commonly dark, unlike glass in most vitric lithic fragments. Microlitic lithic fragments (Figure 10) are defined as 25 - 50% glass, 50 - 75% subhedral to euhedral microlites in the matrix.

Lathwork (Lvl)

Lathwork lithic fragments (Figure 11) contain 50 - 95% glass and 5 - 50% subhedral to euhedral microlites in the matrix. Identification of glass rich lathwork lithic fragments and vitric lithic fragments can be difficult in samples where the glass has been altered. Both felsic (clear) and mafic (dark brown/black) lithic fragments with glass contents greater than 95% are considered vitric lithic fragments (after Marsaglia, 1993).

Aggregate (Lva) and Submicrolitic (Lvsm)

At this point, I propose the introduction of two lithic fragment category subdivisions. The first is the *aggregate volcanic lithic fragment* (Lva, Figure 12). Because the seriate lithic category in Ingersoll and Cavazza's (1991) study is so broad, it seems appropriate to divide it. I propose that aggregate lithic fragments contain 5 - 50% subhedral microlites, 0% glass, and 50 - 100% euhedral microlites in the matrix, with seriate lithic fragments being 50 - 100% subhedral microlites, 0 - 5% glass, and 0 - 50%

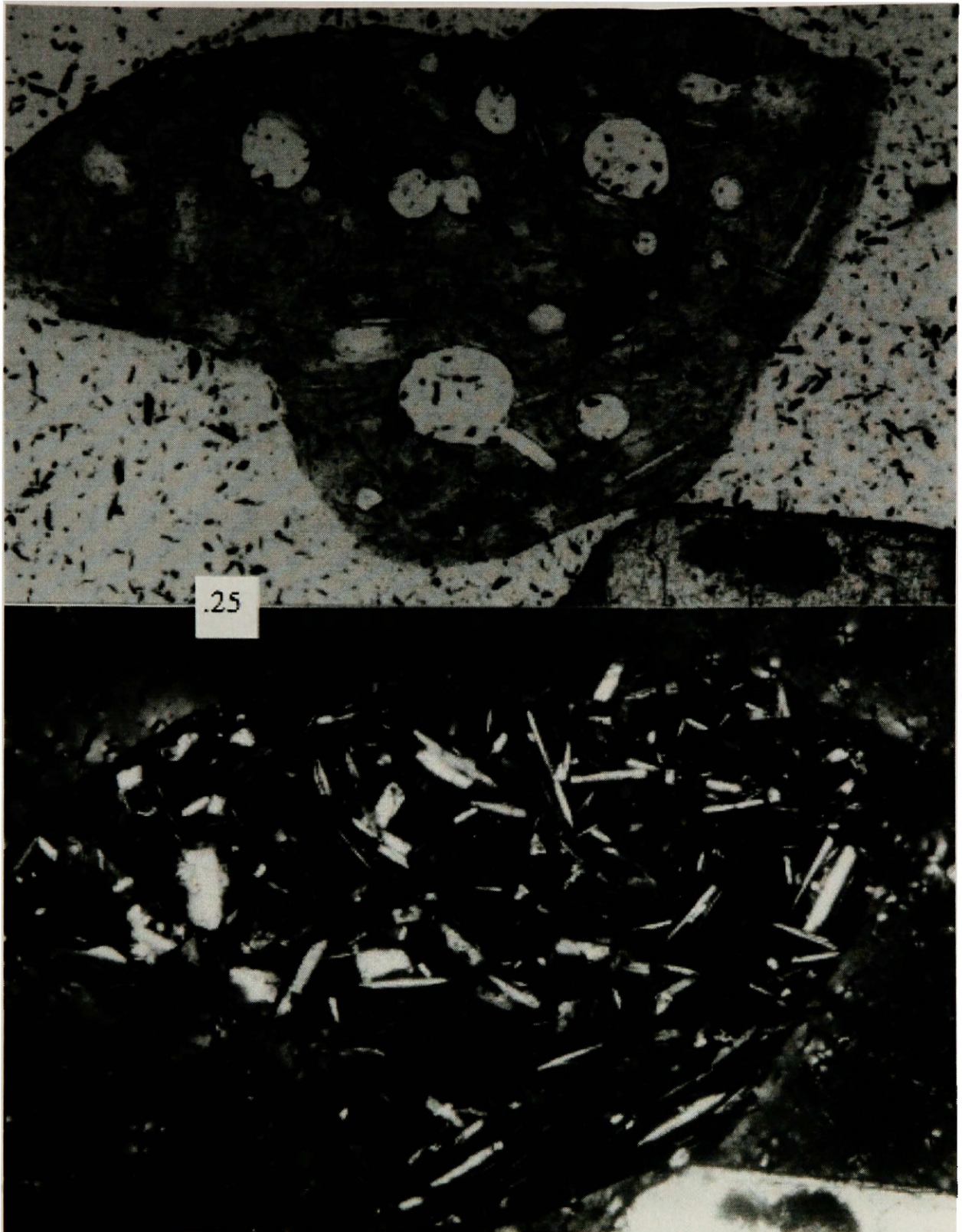


Figure 10. Vesiculated microlitic lithic fragment, made of approximately 40% glass and 60% subhedral and euhedral microlites. From modern sand of Red Hill cinder Cone Quaternary basalt, Coso Volcanic field, California. COS 1A-m, 40X, ppl (A) and xpl (B). Square is 0.25 mm across.

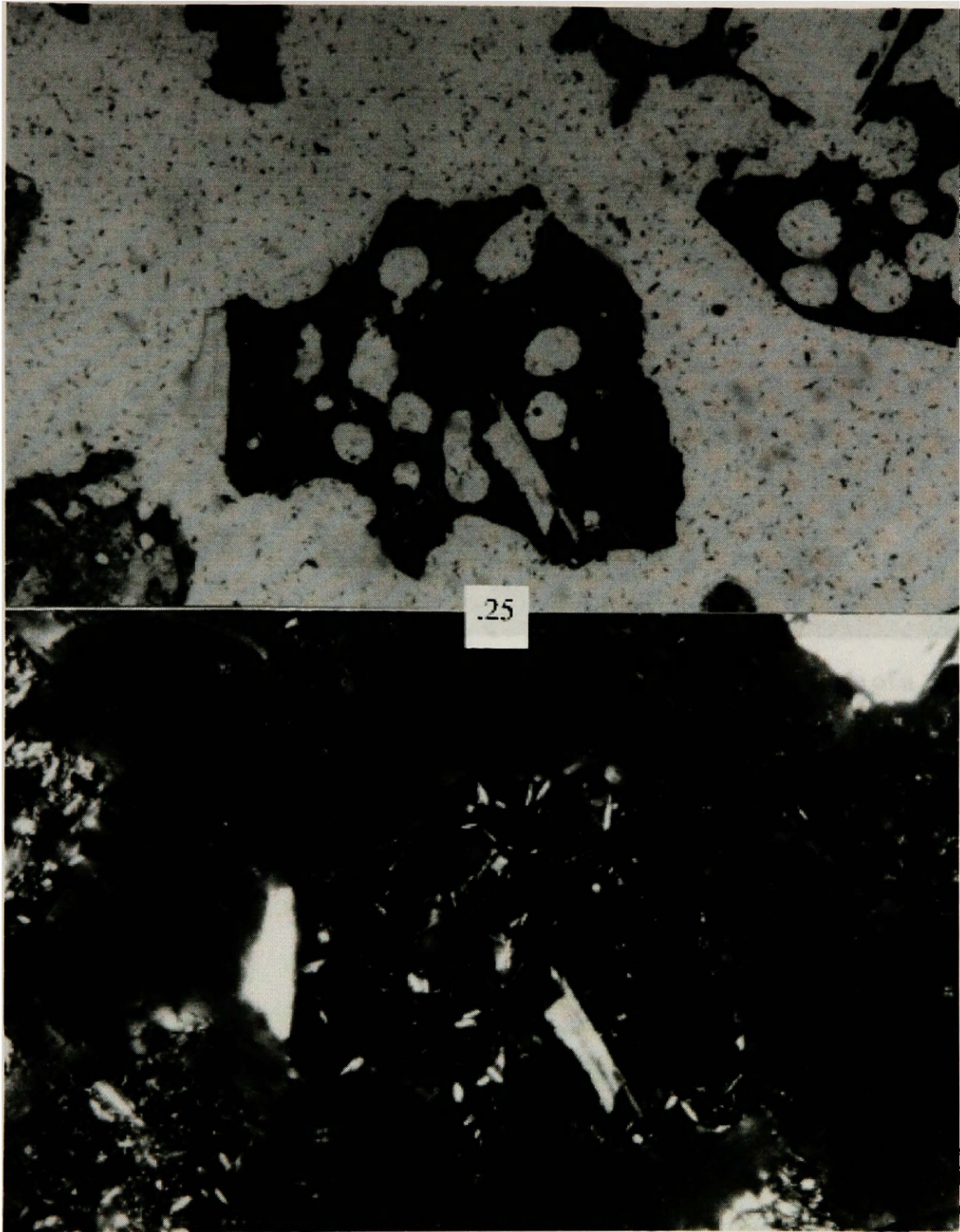


Figure 11. Vesiculated and oxidized lathwork lithic fragment (center), made of approximately 15% euhedral and subhedral microlites and 85% glass. This grain also contains two plagioclase feldspar phenocrysts on left and lower center. From modern sand of Red Hill cinder Cone Quaternary basalt, Coso Volcanic field, California. COS 1A-m, 40X, ppl (A) and xpl (B). Square is 0.25 mm across.

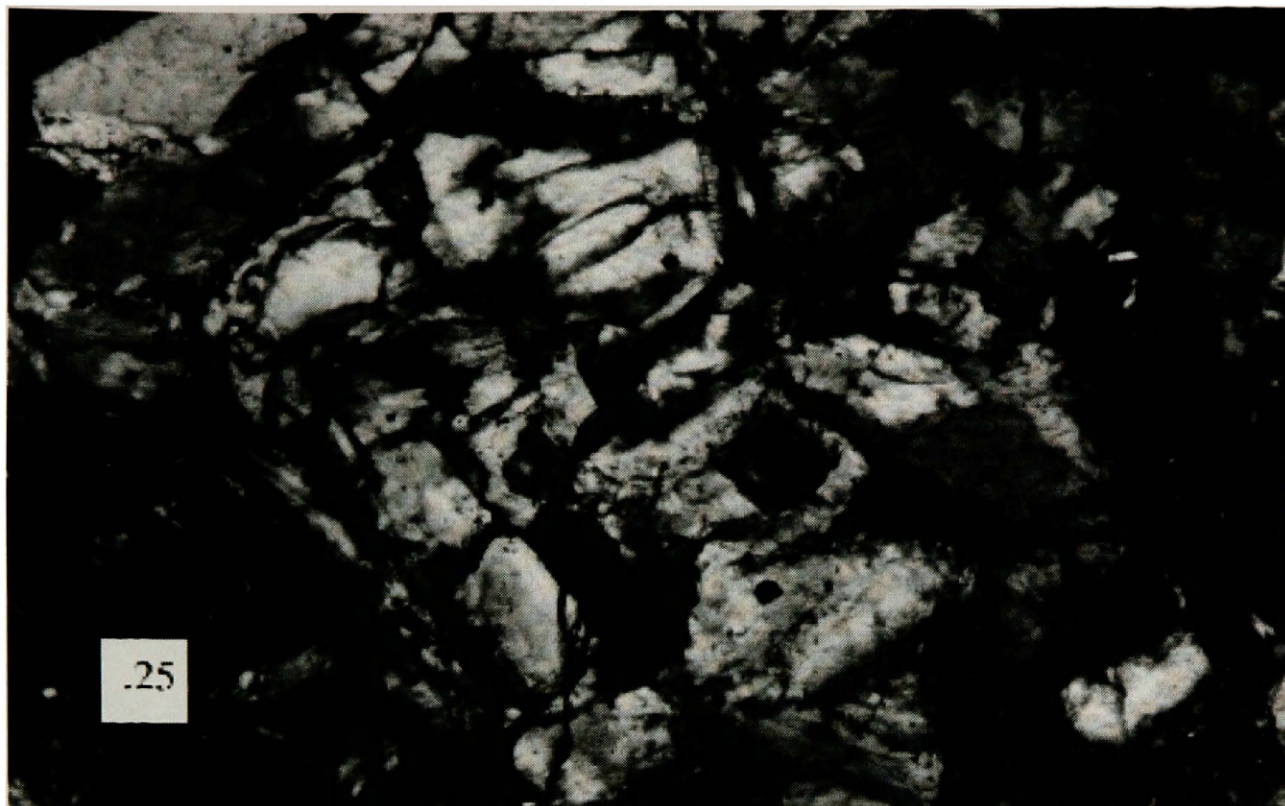


Figure 12. Aggregate lithic material (possible future lithic fragment), made of a cluster of mafic minerals. From a Holocene basalt from Martinique, Lesser Antilles. M8328, 40X, xpl. Square is 0.25 mm across.

euhedral microlites in the matrix. Aggregate lithic fragments are generally formed from cumulates or other crystal clusters, common to intergranular or intersertal igneous textures (Williams et al., 1954). In practice, these are rare in actual sands but can be common in volcanic rocks. The second newly proposed subdivision is the *submicrolitic volcanic lithic fragment* (Lvsm, Figure 13). These are similar to microlitic lithic fragments with glass compositions between 5 and 25%. Definition of this new submicrolitic category helps narrow the definition of the broad microlitic volcanic lithic category. Submicrolitic lithic fragments are defined to have 5 - 25% glass, 75 - 95% subhedral to euhedral microlites in the matrix, with microlitic lithic fragments being 25 - 50% glass and 50 - 75% subhedral to euhedral microlites in the matrix.

Advantages to the New System

Classifying volcanic lithic fragments as I am proposing herein has several advantages. First of all, it covers almost all possible volcanic lithic fragments. If new boundaries, new lithic categories, and/or new matrix crystalline textural types are needed, they could be defined easily without disrupting the entire system, because they would require only slight, specific modifications to existing guidelines. Also, because this system amounts to a more specific version of the past volcanic lithic fragment system established by Ingersoll and Cavazza (1991), only a small percentage of common volcanic lithic fragments would be reclassified from the old system to another category in this new system. Thirdly, the new system eliminates the need for seriate lithic fragments to be a 'garbage' lithic category that includes volcanic lithic fragments that could not be previously placed into a category. Finally, each lithic fragment category has a real, defined boundary, which makes lithic fragment determination less subjective.

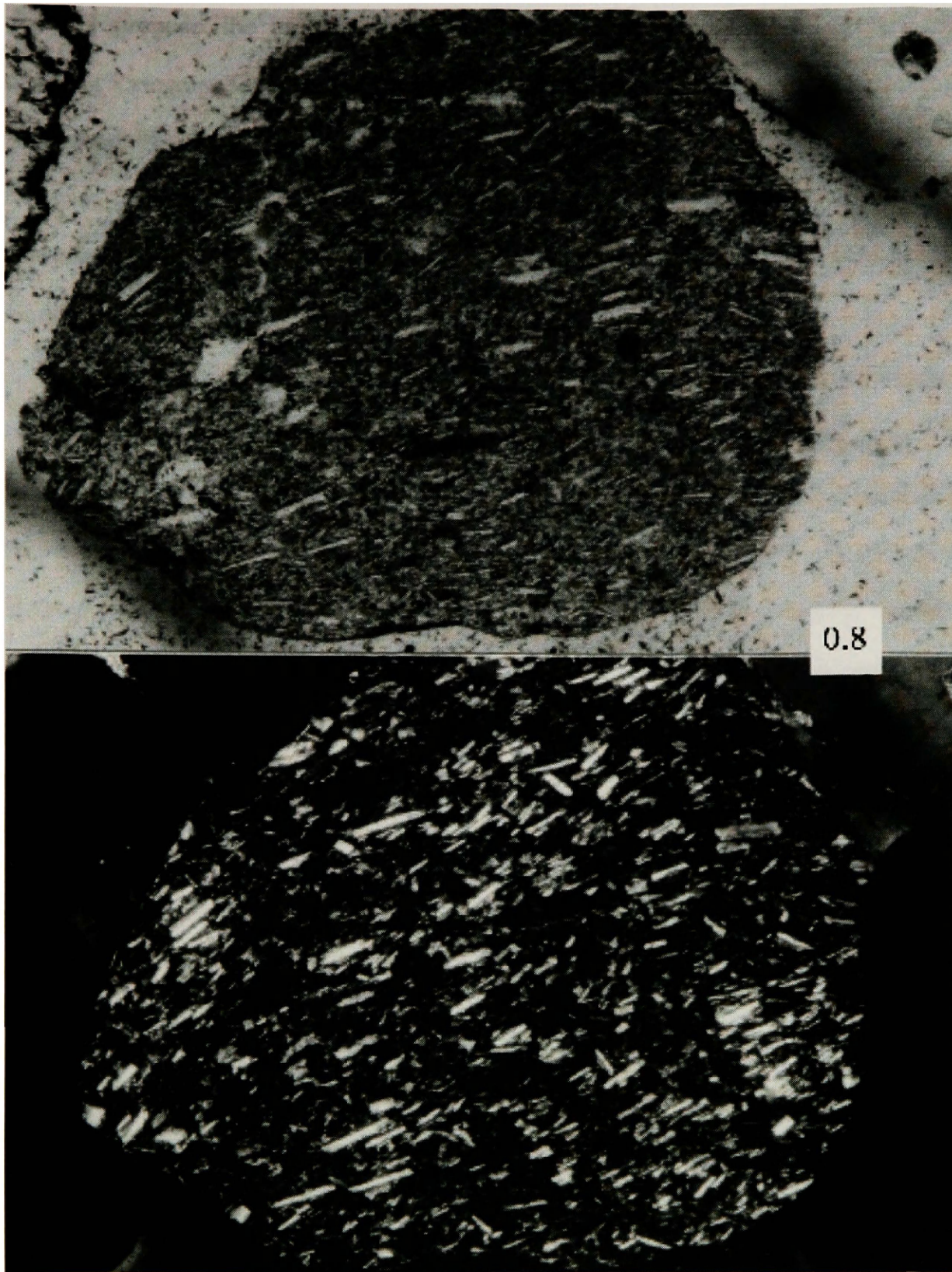


Figure 13. Submicrolitic lithic fragment, made of approximately 85% euhedral and subhedral microlites and 15% glass. From modern sand, Bishop Tuff. BT 1D-m, 12.5X, ppl (A) and xpl (B). Square is 0.80 mm across.

I propose the use of *unidentified volcanic lithic fragments* (Lvu) as a point counting category for lithic fragments that do not fall into one of the previously mentioned lithic fragment categories. The use of this category is likely to be very limited, however, because most volcanic lithic fragments are now easily included in one of the formally defined categories. Any new lithic fragment categories that may be needed could be added to the current system in future work.

The best aspect of this classification scheme is the fact that it does not require any mineralogical information; it depends only on general crystal form and style. As a sedimentary geologist, it is often more pertinent to know about the physical properties of the volcanics that contributed volcanic lithic fragments to the system. In the previous system (Dickinson, 1970; Ingersoll and Cavazza, 1991), cooling history, exotic lava types, and various other factors could have a significant impact on the type of lithic fragments produced, and could render lithic fragments undefinable or mislabeled in a system that only looked at common textures. At a minimum, a system that relates volcanic lithic fragments to the volcanic source rocks would at least have a system which gives an idea of how glassy the volcanic system was, which this system succeeds.

Point Counting Technique

Point counting of zero order samples (Ingersoll, 1990) in this project utilized a modified Gazzi-Dickinson method (Gazzi, 1966; Dickinson, 1970; refined by Ingersoll et al., 1984; Zuffa, 1985; Ingersoll et al., 1993, Table 2). The basic principle is the use of the sand/silt size cutoff as a boundary in the discrimination of monocrystalline and poly(micro)crystalline components of a detrital rock. For example, an individual quartz crystal that is larger than 62.5 μm (0.0625 mm) would be considered monocrystalline

Table 2

Point Count Categories, after Dickinson (1970) and Critelli and Ingersoll (1995).

Qm - crystalline quartz, greater in maximum diameter than .0625 mm.

Qp - polycrystalline (microcrystalline) quartz, with individual crystals smaller than .0625 mm.

K - crystalline feldspar, with an alkali component (non plagioclase), greater in maximum diameter than .0625 mm.

P - crystalline feldspar without an alkali component (plagioclase), greater in maximum diameter than .0625 mm.

M - crystalline mica (including muscovite, biotite, and chlorite), greater in maximum diameter than .0625 mm.

Dpao - crystalline pyroxene, amphibole, and olivine, greater in maximum diameter than .0625 mm.

Dox - crystalline oxides (including magnetite and ilmenite), greater in maximum diameter than .0625 mm.

Ls - microcrystalline (<.0625 mm) rock fragment of sedimentary origin.

Lm - microcrystalline (<.0625 mm) rock fragment of metamorphic origin.

Lvv - volcanic microcrystalline (<.0625 mm) rock fragment with a vitric texture.

Lvg - volcanic microcrystalline (<.0625 mm) rock fragment with a granular texture.

Lvs - volcanic microcrystalline (<.0625 mm) rock fragment with a seriate texture.

Lva - volcanic microcrystalline (<.0625 mm) rock fragment with an aggregate texture.

Lvsm - volcanic microcrystalline (<.0625 mm) rock fragment with a submicrolitic texture.

Lvm - volcanic microcrystalline (<.0625 mm) rock fragment with a microlitic texture.

Lvl - volcanic microcrystalline (<.0625 mm) rock fragment with a lathwork texture.

Lvu - volcanic microcrystalline (<.0625 mm) rock fragment with a texture not described or not within the boundaries of the other volcanic lithic categories.

O - 'other' grain or crystal, not important to overall count. Can include Lm, Ls, Lvu, plant fragments, other minerals (secondary calcite, alkalic minerals), etc.

U - unidentified grain or crystal. By rule, this does not exceed 5% of the count.

(Qm), while a quartz crystal that is smaller than 62.5 μm would be considered part of a larger sand-sized grain (e.g. polycrystalline quartz, chert, various lithic fragments). This is the only system that could produce statistically valid results.

The Gazzi-Dickinson technique had to be modified for this project, because I dealt with volcanic rocks (zero order samples) as opposed to volcanic lithic arenites (first or higher order samples). Upon examining a volcanic rock, I first determined whether the cross-hairs landed on a phenocryst phase (greater than silt-sized) or matrix. If the cross hairs landed on a crystal larger than silt-size, I tabulated it as a monocrystalline grain. If the cross-hairs landed on matrix or a crystal smaller than sand-sized, I determined the proportions of matrix types of the non-phenocryst phase. The modern sand samples I used in this project (see below) were counted using the normal Gazzi-Dickinson method (Gazzi, 1966; Dickinson, 1970; refined by Ingersoll et al., 1984; Zuffa, 1985; Ingersoll et al., 1993). I point counted thin sections between July 2003 and May 2004.

If the cross-hairs landed on area of matrix in a volcanic rock, I took several steps to determine its grain type (after Ingersoll and Cavazza, 1991). In many cases, volcanic rocks have a very homogeneous texture (Figure 14). In such a situation, I examined a ~1 mm wide area to determine the matrix crystalline type proportions (glass, anhedral, subhedral, euhedral) and the corresponding lithic type that would apply if a sand grain were formed from this area of the volcanic rock. I used 1 mm cutoff because this is the standard point count size used to minimize grain size effects on composition in sandstones (Ingersoll et al., 1984). If recognizably different textures occur within the same 1 mm area, than the classification is based upon the textural area that the cross hair lands on, as long as it is within the sand size fraction (Figure 15). If the texture occurs in an area smaller than sand-sized, then it would considered an inclusion in a larger volcanic

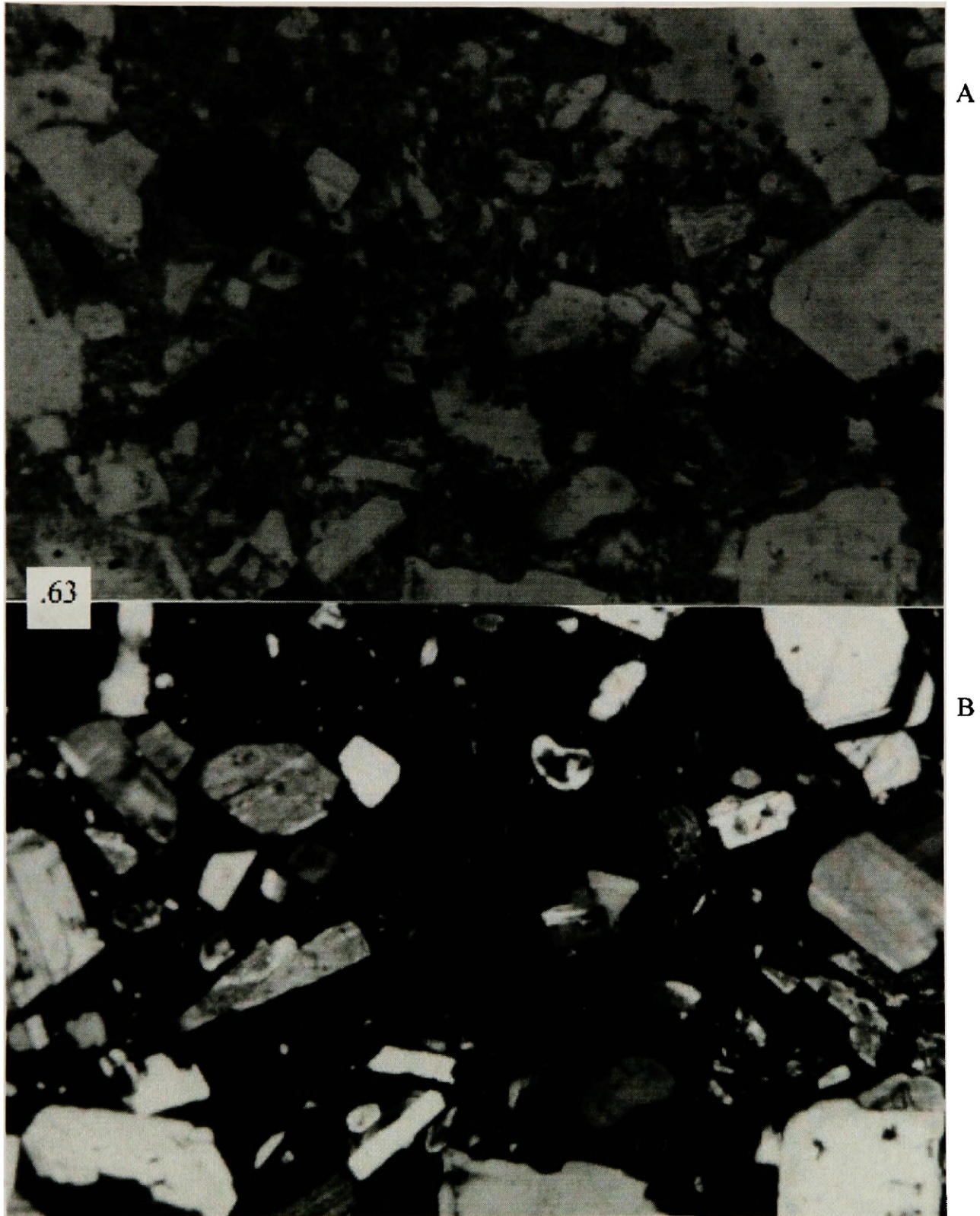


Figure 14. Homogeneous matrix (Lvl). Holocene high silica (65.98) andesite from St. Lucia island, Lesser Antilles. SL8312, 16X, ppl (A) and xpl (B). Square is 1.0 mm across.

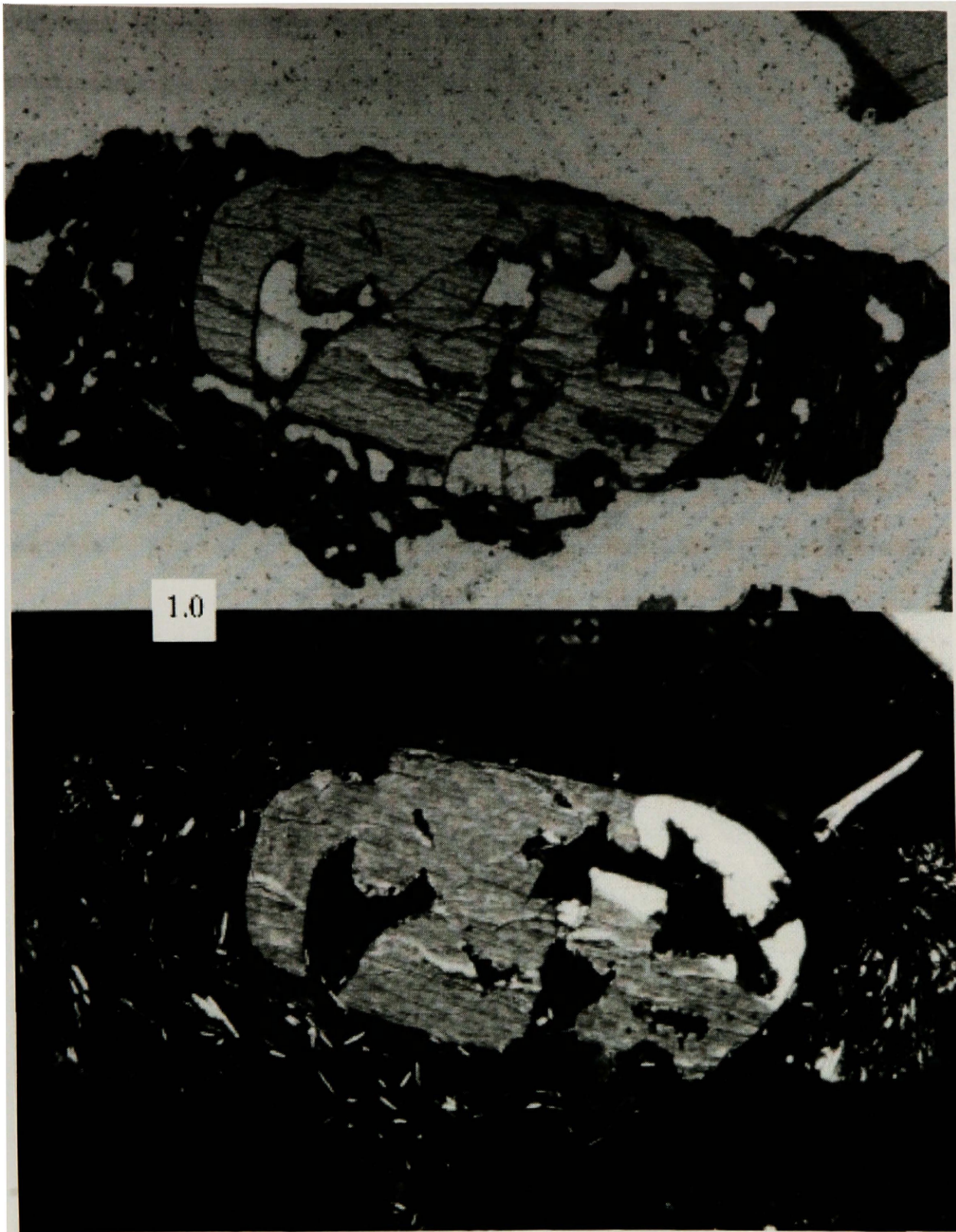


Figure 15. Heterogeneous matrix in a volcanic lithic fragment, with both Lvl (left) and Lvsm (far right) material within the same grain. Modern sand from the Bishop Tuff. BT 1A-m, 10X, ppl (A) and xpl (B). Square is 1.0 mm across.

lithic area. In order to have an understanding of the reproducibility and accuracy of this point counting technique, I point counted a sample of modern sand from the Red Hill basalt in the Coso Volcanic field (Table 3, Figure 16). Overall, the variation was manageable relative to the proposed variation in this Binomial system (Van Der Plas and Tobi, 1965), even though the replications failed a chi-squared test. This shows the large amount of natural variation and difficulty in each point count. Despite the fact that standard point counting procedures were used, the variation was higher than expected, meaning reproducibility is in question, along with the application of the binomial distribution towards point counting in general. Another possibility for the failure of the chi-squared test is the failure of the homogeneous assumption in the sample chosen.

Localities and Sampling

For this study, I borrowed zero order samples (volcanic rocks) from various sources (Table 4), including Jon Davidson, Todd Feeley, John Hora, Bob Christiansen, and the University of Montana thesis collections. Samples were taken from various geographic localities from across the globe, including Montana, Wyoming, New Zealand, islands of the Lesser Antilles, and Yellowstone National Park. The only criteria for selection of a useable sample was that it was a fine grained igneous rock (extrusive or hypabyssal) with known whole rock geochemistry.

First order samples (as defined by Ingersoll, 1990; Ingersoll et al., 1993) were taken from two localities, the Owens River Gorge near Bishop, CA (Figure 17) and Red Hill near Little Lake, CA (Figure 16). The Owens River Gorge cuts through the .76 Ma Bishop Tuff which has a whole rock weight %SiO₂ of 75.5 to 77.6 (Hildreth, 1977; Anderson et al., 2000). The Owens River samples (BT1a through BT1d) were collected

Table 3

Point Count Replication Data and Statistics

Since point counting theoretically represents a binomial distribution (Van der Plas and Tobi, 1965), the goodness of fit to a binomial distribution with population parameters estimated from the data is used in order to test the reproducibility of the counts used in this thesis (after Zar, 1999). Sample COS 1A-m was used because of its small grain size (to reduce multiple counts on the same grain), diverse volcanic lithic fragment population, and ease of counting (equal thickness across slide, lack of felsic minerals other than plagioclase feldspar, etc.). I performed chi-squared tests on all six frequently occurring parameters (> 3 grains per sample) in COS 1A-m. Table 3.1 shows the data for these 5 counts (1 for data collection and 4 replications).

Table 3.1

Replication #	Date	P	Lvv	Lvsm	Lvm	Lvl	Dpao	Total points
initial*	2-21	91	27	25	68	137	49	400
1	3-25	95	33	37	86	163	86	500
2	4-6	116	22	46	70	179	60	500
3	4-7	122	15	30	68	172	87	500
4	4-8	91	17	42	91	173	83	500

*Note: the initial count was only 400 points, while the replications were 500 points each. The initial count was used in some calculations (p-hat) but not the chi-squared test.

First I estimated p-hat, the estimate from the data of the population parameter p, the theoretical percentage of each parameter in the population. This is calculated from the total sum of each element divided by the total points counted (2,400). I also calculated q-hat (1 - p-hat), x-exp (the average number of grains found in each 500 point sample based on p-hat, rounded to the nearest grain), s (the standard deviation of the 4 replication counts for each parameter), and sigma (theoretical standard deviation of each parameter based on binomial distribution, \sqrt{npq}). Table 3.2 (below) shows this information.

Table 3 (cont.)

Table 3.2

	P	Lvv	Lvsm	Lvm	Lvl	Dpao
p-hat	0.215	0.0475	0.0750	0.160	0.343	0.152
q-hat	0.785	0.9525	0.925	0.840	0.657	0.848
x-exp	108	24	38	80	172	76
s	13.2	6.98	5.97	9.93	5.72	11.1
sigma	9.19	4.76	5.89	8.20	10.6	8.03

Taking the parameter with the highest standard deviation in the data, P, and using the fact that $\sigma = 9.19$, we see that the sample standard deviation is much less than 2-sigma, which would lead to the conclusion that the data fits within the normal variation about the chi-squared distribution. In cases like Lvl, the sample standard deviation is 1/2 sigma. Also, the glass factors (see discussion on pg. 44) of the four replications are 0.5898, 0.5764, 0.5902, and 0.5593, which also supports the replication potential of this technique (the original count also gave a close 0.6528 for the glass factor).

In order to confirm the qualitative analysis of the previous paragraph, I performed a quantitative statistical analysis known as a chi-squared test. This is done by examining the chi-squared distribution and by calculating a chi-squared statistic based upon the equation:

$$\sum_{i=1}^R \sum_{j=1}^C \frac{(O_{ij} - E_{ij})^2}{E_{ij}}$$

where O_{ij} is the observed value in each cell (of table 3.1), E_{ij} is the the expected (theoretical) value (x-exp from Table 12.2) for each cell, and the cells are identified by their row number i (1 to R) and column number j (1 to C). I calculated this number to be 34.258. The degrees of freedom for this calculation is equal to $(R-1)*(C-1)$ which is 15. So, a chi-squared distribution with 15 degrees of freedom and a value of 34.258 gives a probability of being equal or more extreme of .0031342 or less. The 5% cutoff for this distribution is 24.996. This leads to the conclusion that while the point counting in this thesis seems reliable based on estimates of sigma, it is not statistically reproducible. The difficulty in point counting, the inherent subjective nature of point counting, and the number of assumptions built into a point count (homogeneously distributed grains) may have added to this result. This result questions the use of the binomial distribution in point counting in general.

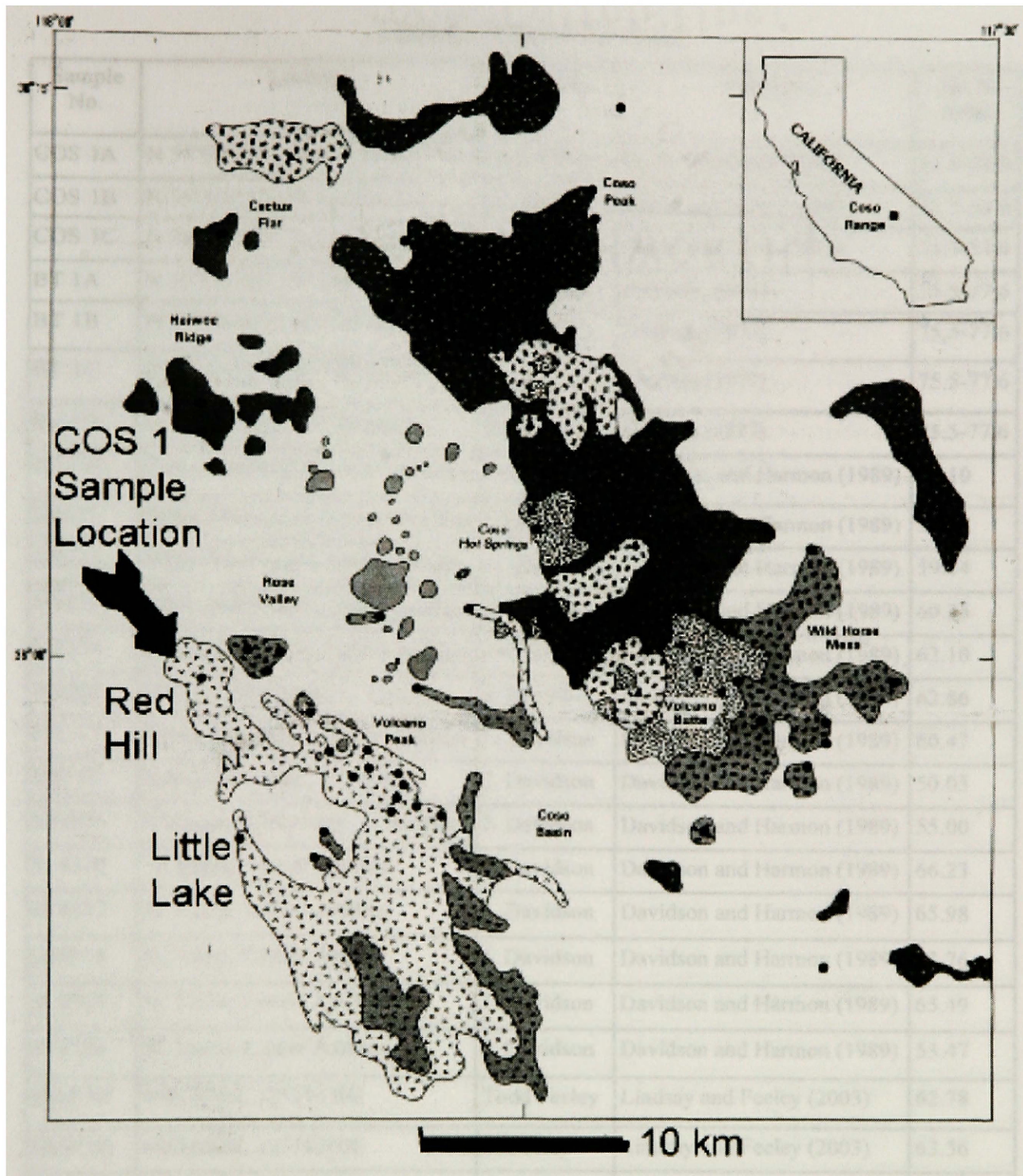


Figure 16. Map of the Coso range volcanic field, showing the location of Red Hill, where samples COS 1A - COS 1C were collected. Scale bar is 10 km. From Novak and Bacon (1986).

Table 4 - Sample Database

Sample No.	Location	Supplier	Reference	wt. % SiO ₂
COS 1A	N 35°59.232', W 117°54.751'	Matt Affolter	Bacon and Metz (1984)	51.7-54.0
COS 1B	N 35°59.317', W 117°54.375'	M. Affolter	Bacon and Metz (1984)	51.7-54.0
COS 1C	N 35°59.378', W 117°54.252'	M. Affolter	Bacon and Metz (1984)	51.7-54.0
BT 1A	N 37°30.105', W 118°34.068'	M. Affolter	Hildreth (1977)	75.5-77.6
BT 1B	N 37°30.462', W 118°34.117'	M. Affolter	Hildreth (1977)	75.5-77.6
BT 1C	N 37°30.981', W 118°34.292'	M. Affolter	Hildreth (1977)	75.5-77.6
BT 1D	N 37°30.082', W 118°34.350'	M. Affolter	Hildreth (1977)	75.5-77.6
M8214	Pelee, Martinique, Lesser Antilles	Jon Davidson	Davidson and Harmon (1989)	61.10
M8217	Pelee, Martinique, Lesser Antilles	J. Davidson	Davidson and Harmon (1989)	58.94
M8222	Pelee, Martinique, Lesser Antilles	J. Davidson	Davidson and Harmon (1989)	59.14
M8225	Pelee, Martinique, Lesser Antilles	J. Davidson	Davidson and Harmon (1989)	60.26
M8228	Pelee, Martinique, Lesser Antilles	J. Davidson	Davidson and Harmon (1989)	62.10
M8268	Carbet, Martinique, L. Antilles	J. Davidson	Davidson and Harmon (1989)	62.86
M8277	Pelee, Martinique, Lesser Antilles	J. Davidson	Davidson and Harmon (1989)	60.47
M8310	submarine, Mart., L. Antilles	J. Davidson	Davidson and Harmon (1989)	50.03
M8328	Diamant, Martinique, L. Antilles	J. Davidson	Davidson and Harmon (1989)	55.00
SL8308	St. Lucia, Lesser Antilles	J. Davidson	Davidson and Harmon (1989)	66.23
SL8312	St. Lucia, Lesser Antilles	J. Davidson	Davidson and Harmon (1989)	65.98
SL8316	St. Lucia, Lesser Antilles	J. Davidson	Davidson and Harmon (1989)	63.76
SL8324	St. Lucia, Lesser Antilles	J. Davidson	Davidson and Harmon (1989)	65.49
SL8326	St. Lucia, Lesser Antilles	J. Davidson	Davidson and Harmon (1989)	53.47
SM9701	4981870N, 12518530E	Todd Feeley	Lindsay and Feeley (2003)	62.78
SM9702	4981600N, 12518360E	T. Feeley	Lindsay and Feeley (2003)	63.56
SM9703	4981480N, 12518260E	T. Feeley	Lindsay and Feeley (2003)	63.71
SM9704	4980520N, 12518340E	T. Feeley	Lindsay and Feeley (2003)	62.85
SM9705	4980740N, 12518380E	T. Feeley	Lindsay and Feeley (2003)	62.09
SM9706	4985240N, 12519910E	T. Feeley	Lindsay and Feeley (2003)	69.35
SM9709	4983910N, 12518450E	T. Feeley	Lindsay and Feeley (2003)	58.01
SM9712	4983410N, 12518280E	T. Feeley	Lindsay and Feeley (2003)	56.27

Table 4 (cont.)

Sample No.	Location	Supplier	Reference	wt. % SiO ₂
SM9713	4977480N, 12518020E	T. Feeley	Lindsay and Feeley (2003)	62.16
SM9715	4978460N, 12517720E	T. Feeley	Lindsay and Feeley (2003)	61.05
SM9716	4978560N, 12517550E	T. Feeley	Lindsay and Feeley (2003)	58.80
SM9717	4978610N, 12517490E	T. Feeley	Lindsay and Feeley (2003)	59.51
SM9718	4982380N, 12518780E	T. Feeley	Lindsay and Feeley (2003)	58.60
SM9719	4981160N, 12518580E	T. Feeley	Lindsay and Feeley (2003)	62.60
SM9720	4981960N, 12518820E	T. Feeley	Lindsay and Feeley (2003)	58.42
SM9721	4982070N, 12518460E	T. Feeley	Lindsay and Feeley (2003)	58.38
SM9722	4982110N, 12518400E	T. Feeley	Lindsay and Feeley (2003)	60.36
SM9724	4982440N, 12518050E	T. Feeley	Lindsay and Feeley (2003)	68.43
SM9725	4982600N, 12517980E	T. Feeley	Lindsay and Feeley (2003)	61.34
SM9726	4982730N, 12517980E	T. Feeley	Lindsay and Feeley (2003)	58.50
SM9727	4982810N, 12517990E	T. Feeley	Lindsay and Feeley (2003)	59.02
SM9730	4986620N, 12517280E	T. Feeley	Lindsay and Feeley (2003)	66.57
SM9731	4986340N, 12516800E	T. Feeley	Lindsay and Feeley (2003)	64.29
SM9732	4986N, 12516E	T. Feeley	Lindsay and Feeley (2003)	65.70
SM9733	4986120N, 12517990E	T. Feeley	Lindsay and Feeley (2003)	65.42
SM9734	4985990N, 12517680E	T. Feeley	Lindsay and Feeley (2003)	67.07
SM9735	4985770N, 12517350E	T. Feeley	Lindsay and Feeley (2003)	68.95
SM9736	4985700N, 12517270E	T. Feeley	Lindsay and Feeley (2003)	59.07
SM9737	4985560N, 12517050E	T. Feeley	Lindsay and Feeley (2003)	57.40
SM9738	4985560N, 12516990E	T. Feeley	Lindsay and Feeley (2003)	62.54
SM9740	4985510N, 12516950E	T. Feeley	Lindsay and Feeley (2003)	63.84
SM9810	4983070N, 12516900E	T. Feeley	Lindsay and Feeley (2003)	64.43
SM9826	4982910N, 1251820E	T. Feeley	Lindsay and Feeley (2003)	58.75
SM9827	4982940N, 12518200E	T. Feeley	Lindsay and Feeley (2003)	57.79
SM9828	4983340N, 12518200E	T. Feeley	Lindsay and Feeley (2003)	55.81
TLC9701	4986630N, 12517410E	T. Feeley	Lindsay and Feeley (2003)	63.83
Tr 191	N 44°15', W 115°15'	UM collection	Luthy (1981)	76.93

Table 4 (cont.)

Sample No.	Location	Supplier	Reference	wt. % SiO ₂
39C	N 48°23', W 108°50'	UM Collection	Leppert (1985)	49.6
32L	N 48°23', W 108°50'	UM	Leppert (1985)	51.68
260A	N 46°45', W 114°30' W	UM	Holloway (1980)	69.20
70A	N 46°45', W 114°30' W	UM	Holloway (1980)	74.80
54A	N 46°45', W 114°30' W	UM	Holloway (1980)	73.22
66A ttf	N 46°45', W 114°30' W	UM	Holloway (1980)	71.00
P39850	Ngauruhoe Volcano, Taupo, NZ	John Hora	Hobden (1997)	55.71
P39864	Ngauruhoe Volcano, Taupo, NZ	J. Hora	Hobden (1997)	55.82
TG001	Ngauruhoe Volcano, Taupo, NZ	J. Hora	Hobden (1997)	55.44
TG004	Ngauruhoe Volcano, Taupo, NZ	J. Hora	Hobden (1997)	55.06
TG010	Ngauruhoe Volcano, Taupo, NZ	J. Hora	Hobden (1997)	56.93
TG019	Ngauruhoe Volcano, Taupo, NZ	J. Hora	Hobden (1997)	56.51
TG041	Ngauruhoe Volcano, Taupo, NZ	J. Hora	Hobden (1997)	55.19
TG043	Ngauruhoe Volcano, Taupo, NZ	J. Hora	Hobden (1997)	56.23
TG540	Ngauruhoe Volcano, Taupo, NZ	J. Hora	Hobden (1997)	56.71
TG575	Ngauruhoe Volcano, Taupo, NZ	J. Hora	Hobden (1997)	55.06

along the Owens River at approximately N 37° 30' W 118° 34' and sieved into coarse (>2.0 mm), medium (2.0 - 0.25 mm), and fine (0.25 - 0.0625 mm) fractions.

The Red Hill Cinder Cone (51.7 to 54.0 wt. %SiO₂, Bacon and Metz, 1984) is part of the Pliocene to Quaternary Coso Volcanic field which separates the Owens Valley to the north and the Indian Wells Valley to the south (Novak and Bacon, 1986). Samples (COS 1a - 1c) were taken from the slopes of the Red Hill Cinder Cone near N 35° 59' W 117° 54' (See Table 4 for exact sample locations).

RESULTS

The data for the 96 point counted thin sections performed in this study are tabulated in Appendix I. In order to reduce the influence of phenocrysts (and their relative abundance) on the overall counts, I normalized each specific volcanic lithic fragment category to the total number of volcanic lithic fragment counted. This percentage I call the *lithic ratio* and is shown on the y axis in Figures 18 - 21. In those figures, I plotted all of the lithic ratio data verses weight % SiO₂ (on the x axis) in the volcanic rock, because wt. % SiO₂ is the standard chemical classification system used for igneous rocks (Williams et al., 1954).

Another valid and more complete way of presenting this data is with a term I call the Glass Factor (%Gf). The %Gf is a proxy for the amount of glass in a particular volcanic rock or suite of volcanic lithic fragments, based upon the proportions of the different volcanic lithic fragments present (Figures 22 - 26). This number is calculated by taking each lithic ratio and multiplying by the theoretical weighted median glass content of the lithic in question (97.5% for Lv_v, 15% for Lv_{sm}, etc.). The results of this calculation are plotted in Figure 22 for the zero order samples and in Figures 23 and 24 for the first

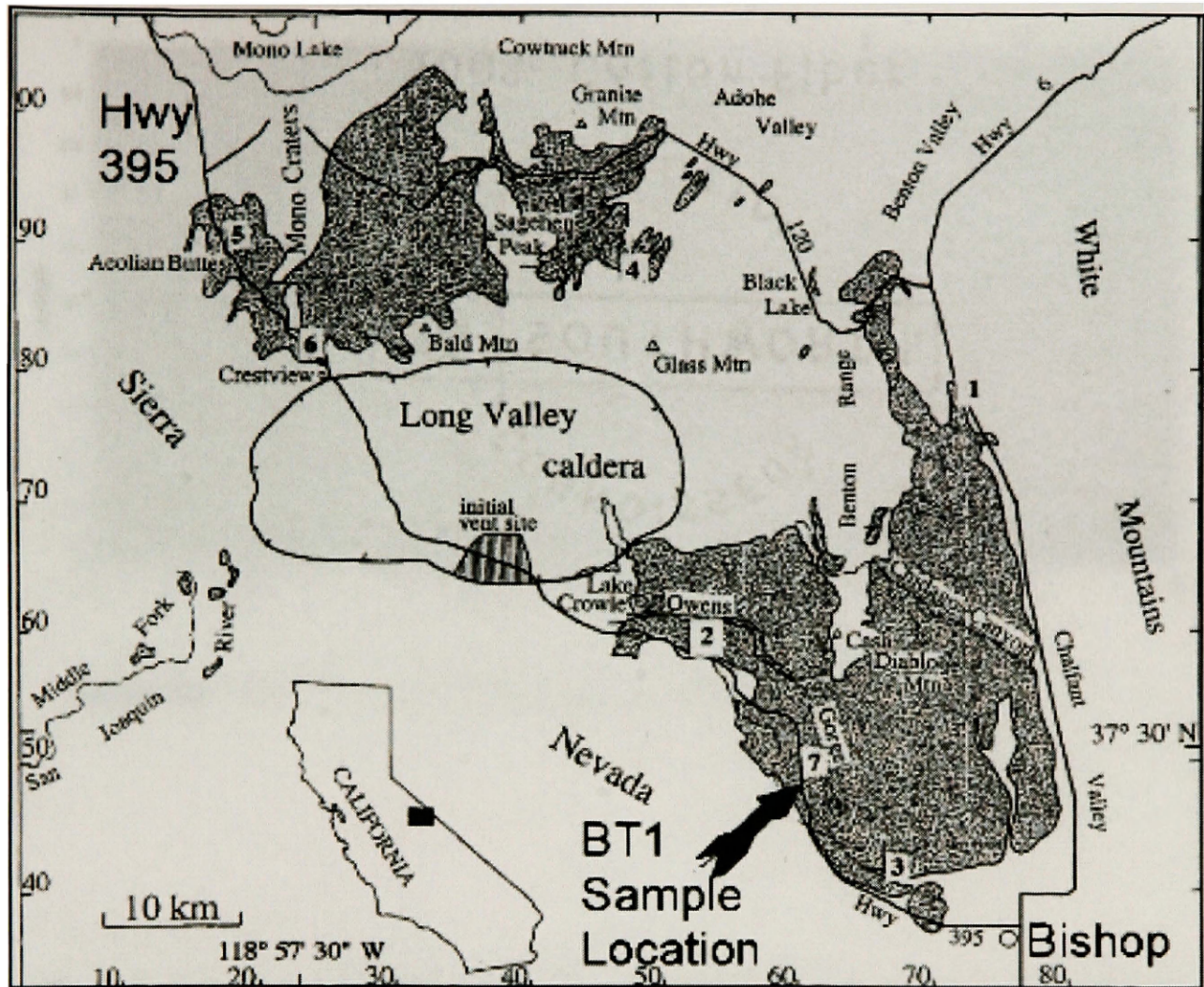


Figure 17. Map of the Bishop Tuff and Long Valley caldera in northern Owens Valley, CA. Arrow indicates approximate location of modern sand BT1A-BT1D collection in the Owens River Gorge. From Anderson et al. (2001).

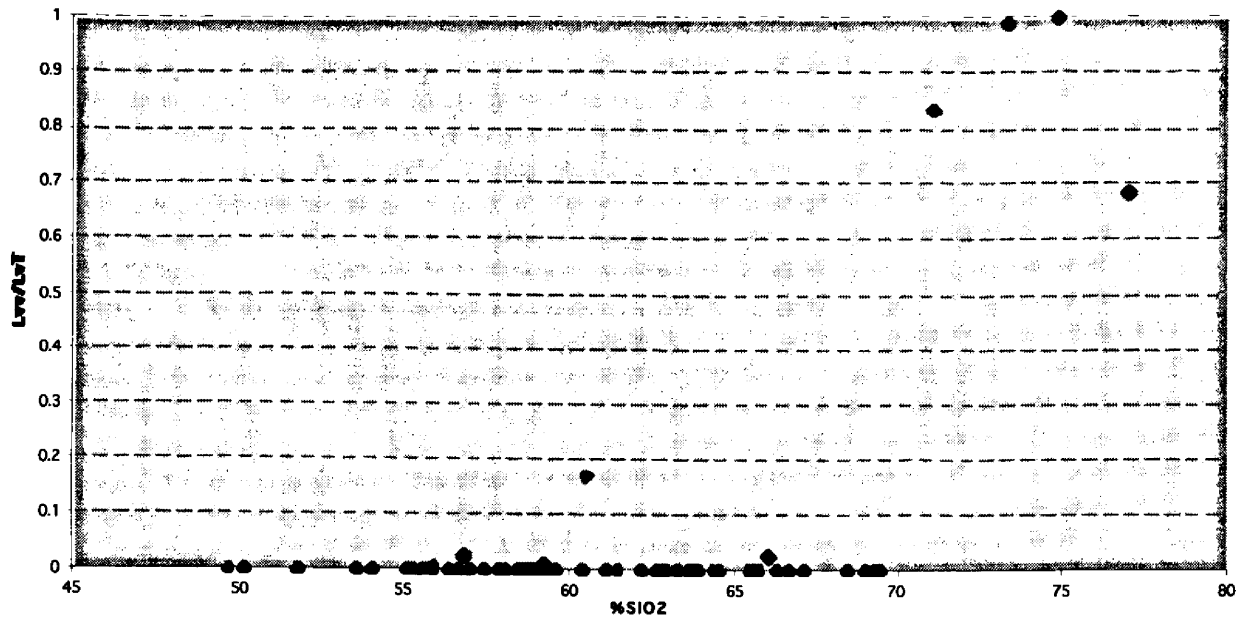


Figure 18a. Plot of L_{vv}/L_{vT} (lithic ratio) vs. wt. % SiO_2 .

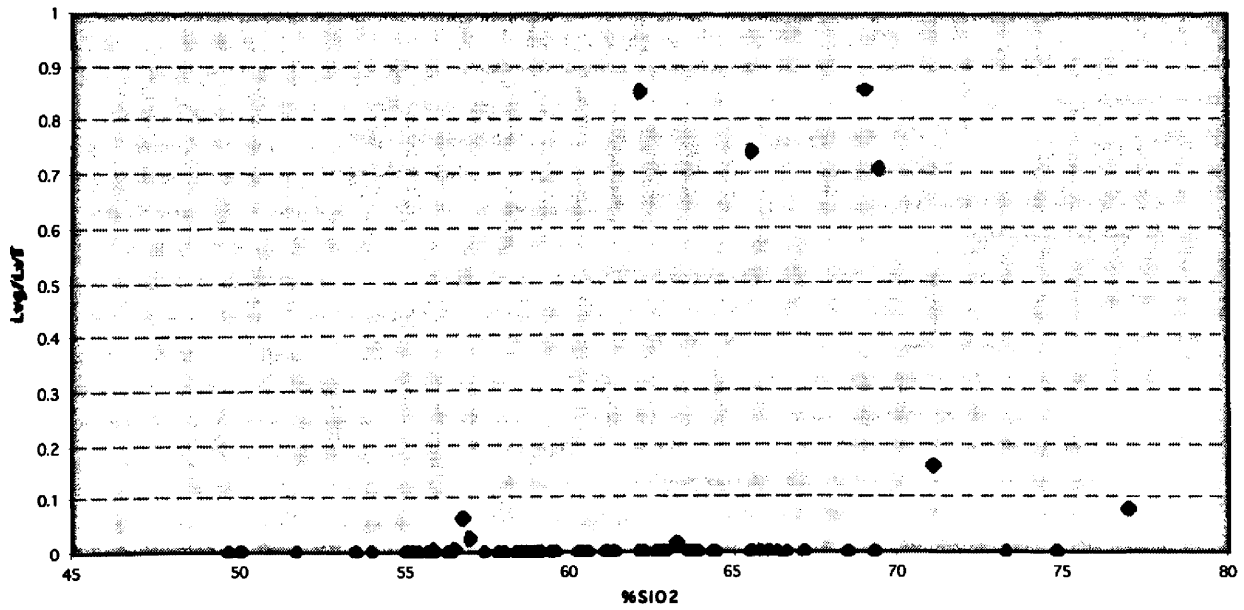


Figure 18b. Plot of L_{vg}/L_{vT} (lithic ratio) vs. wt. % SiO_2 .

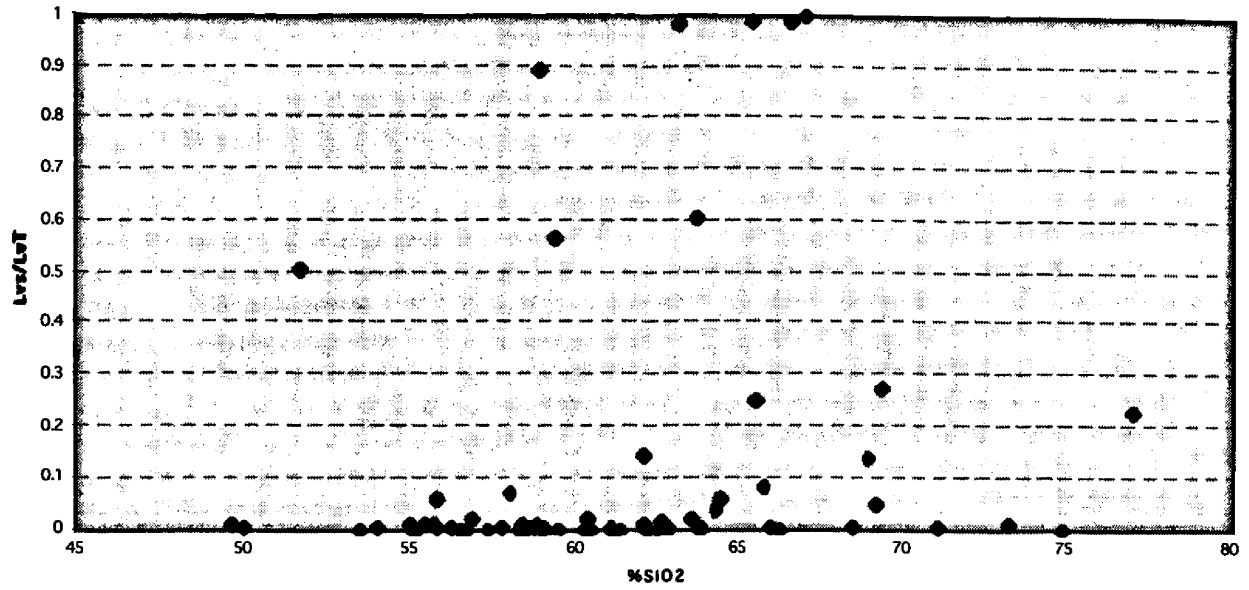


Figure 19a. Plot of Lvs/LvT (lithic ratio) vs. wt. % SiO_2 .

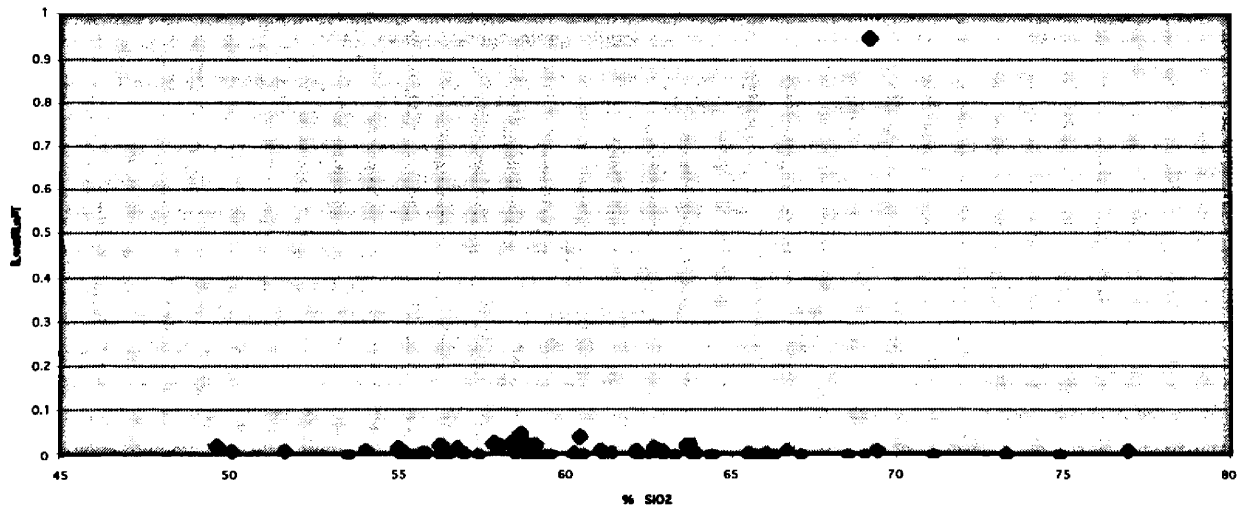


Figure 19b. Plot of Lva/LvT (lithic ratio) vs. wt. % SiO_2 .

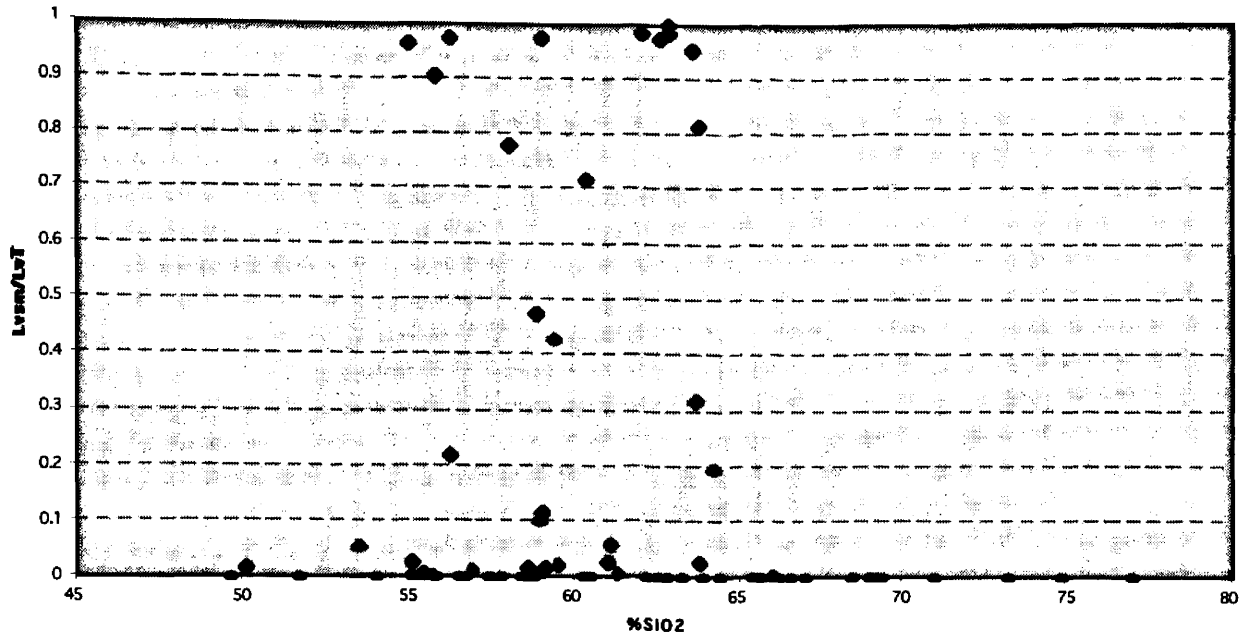


Figure 20a. Plot of $Lvsm/LvT$ (lithic ratio) vs. wt. % SiO_2 .

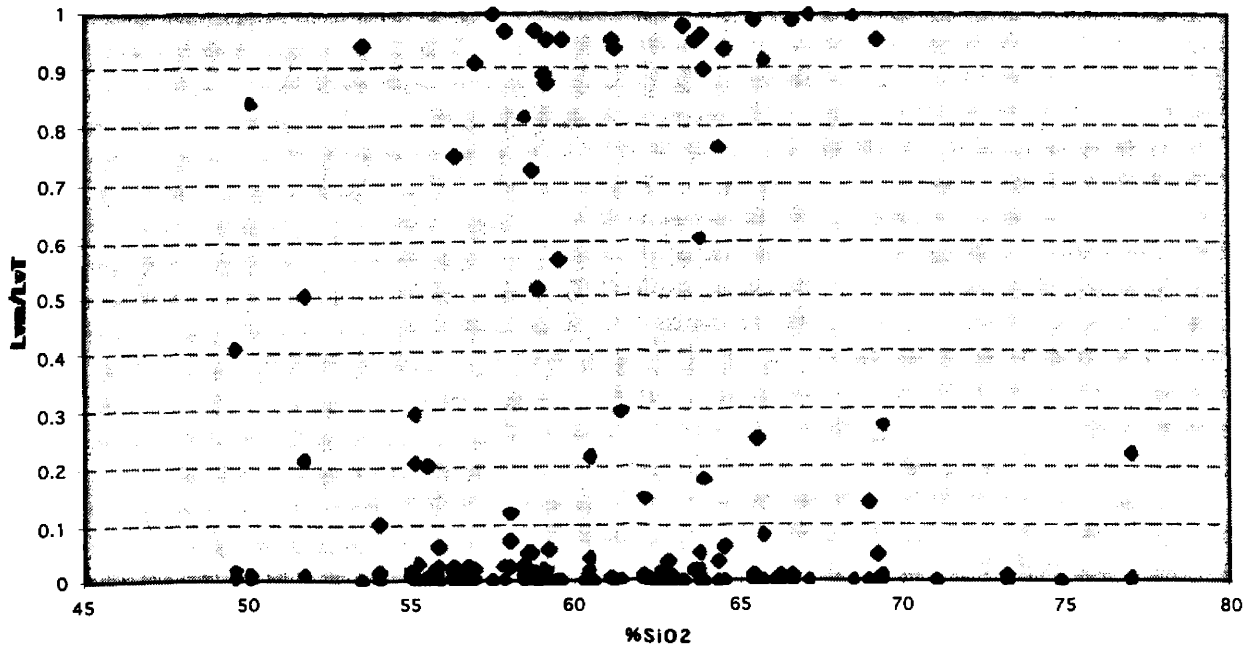


Figure 20b. Plot of Lvm/LvT (lithic ratio) vs. wt. % SiO_2 .

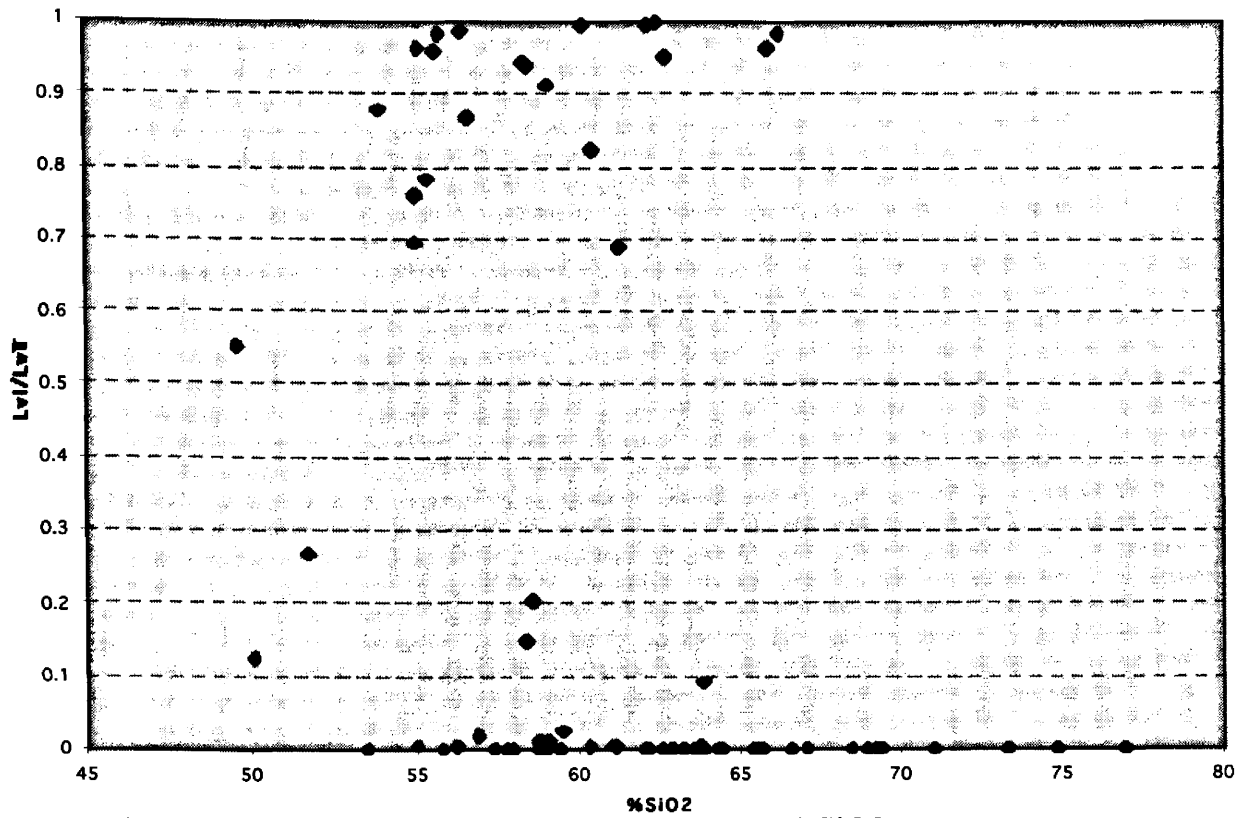


Figure 21. Plot of Lv/LvT (lithic ratio) vs. wt. % SiO2.

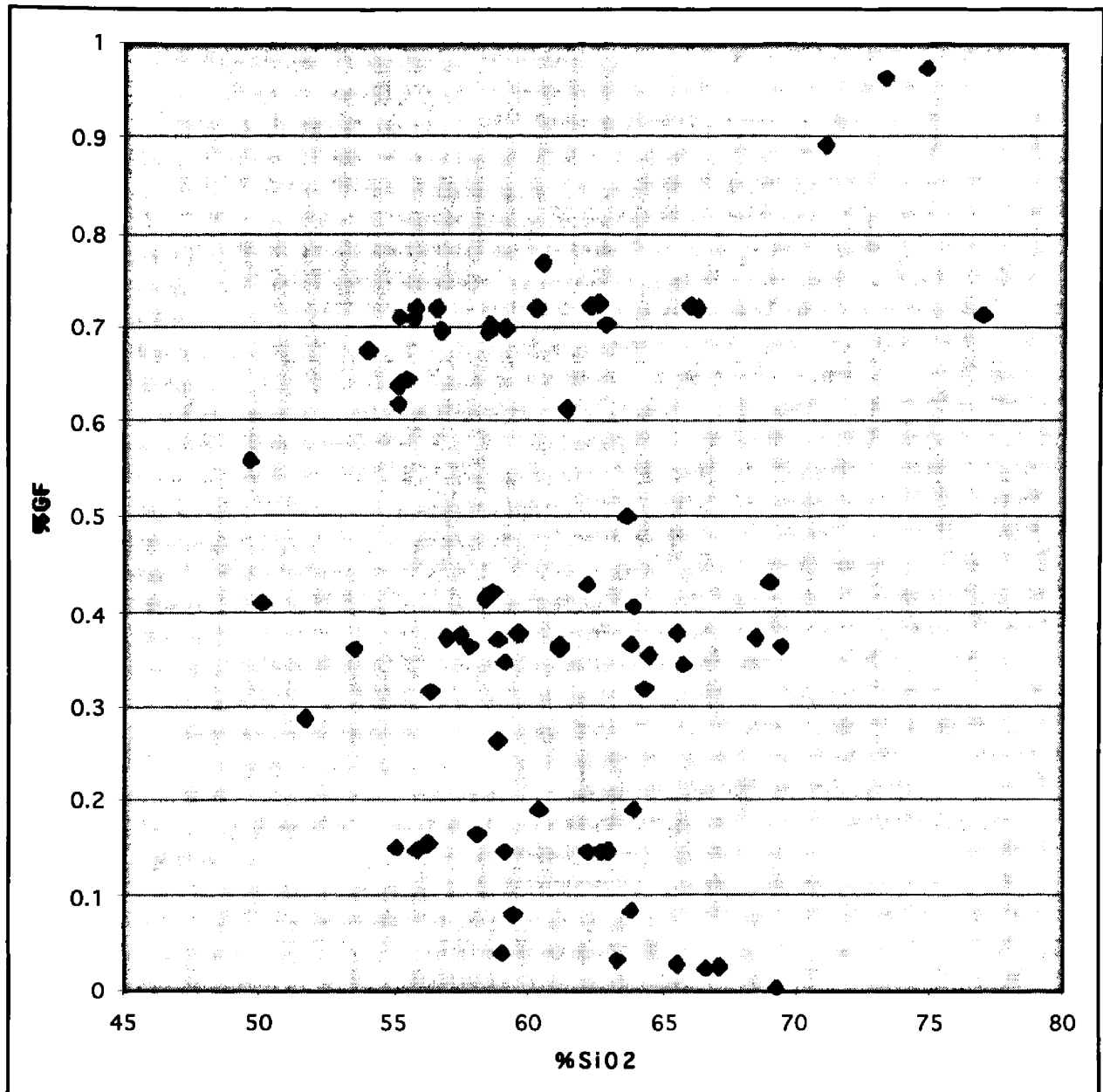


Figure 22. Plot of %Gf vs. wt. % SiO₂ for zero order samples.

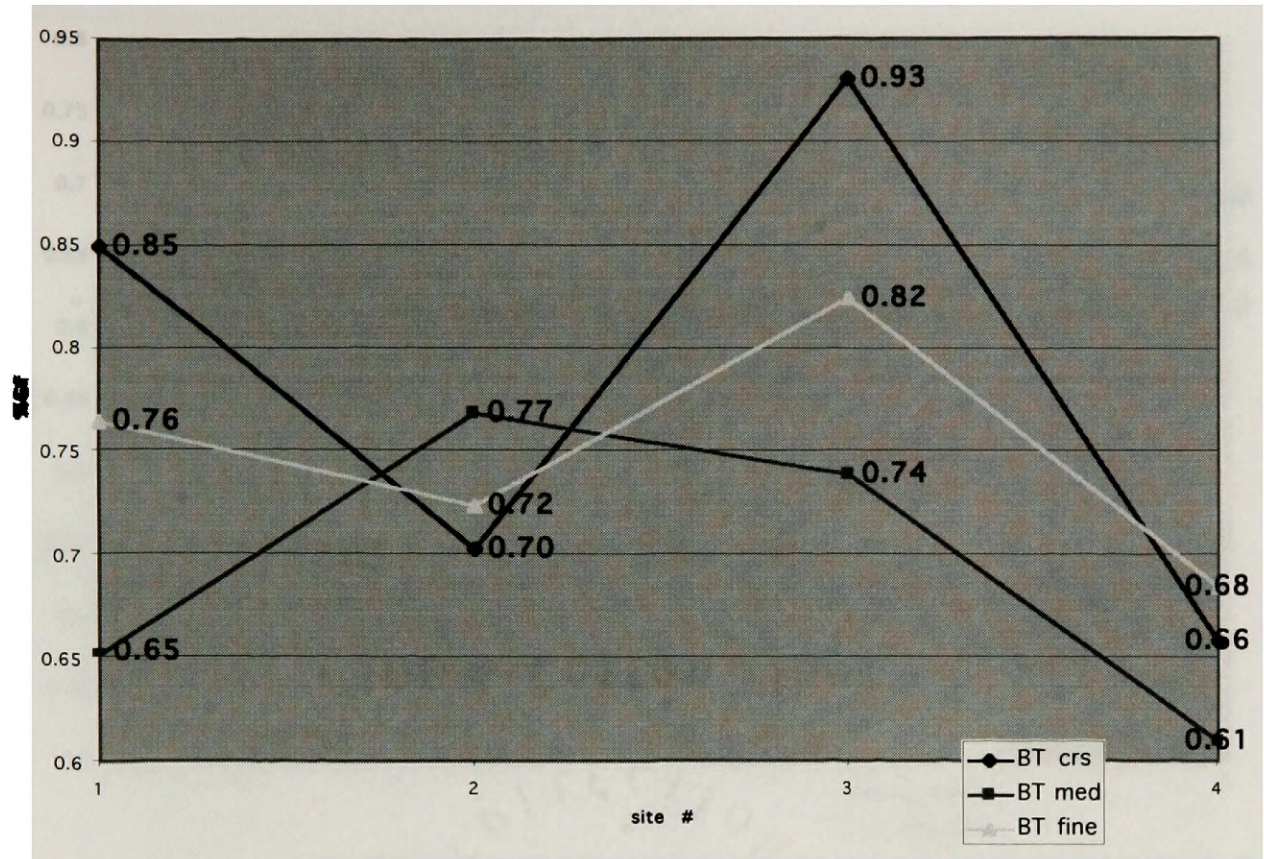


Figure 23. Plot of %Gf vs. sample number (increasing downstream) for Bishop Tuff samples. Data is separated into coarse (> 2 mm), medium (2 mm - 0.25 mm), and fine (0.25 - 0.0625 mm) fractions. Site distance is approximately 1 mile apart each.

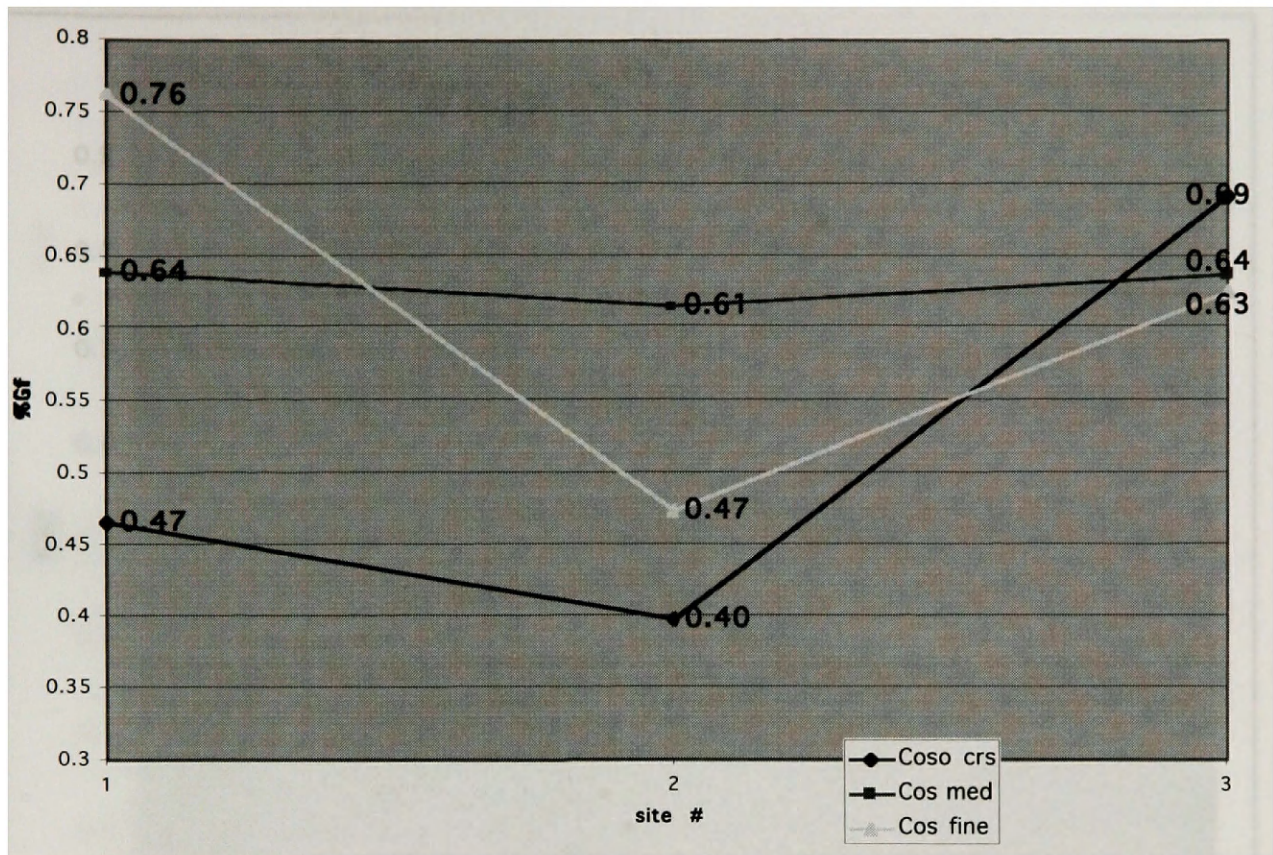


Figure 24. Plot of %Gf vs. sample number (increasing downstream) for Coso volcanic (Red Hill) samples. Data is separated into coarse (> 2 mm), medium (2 mm - 0.25 mm), and fine (0.25 - 0.0625 mm) fractions. Site distance is approximately 1 mile apart each.

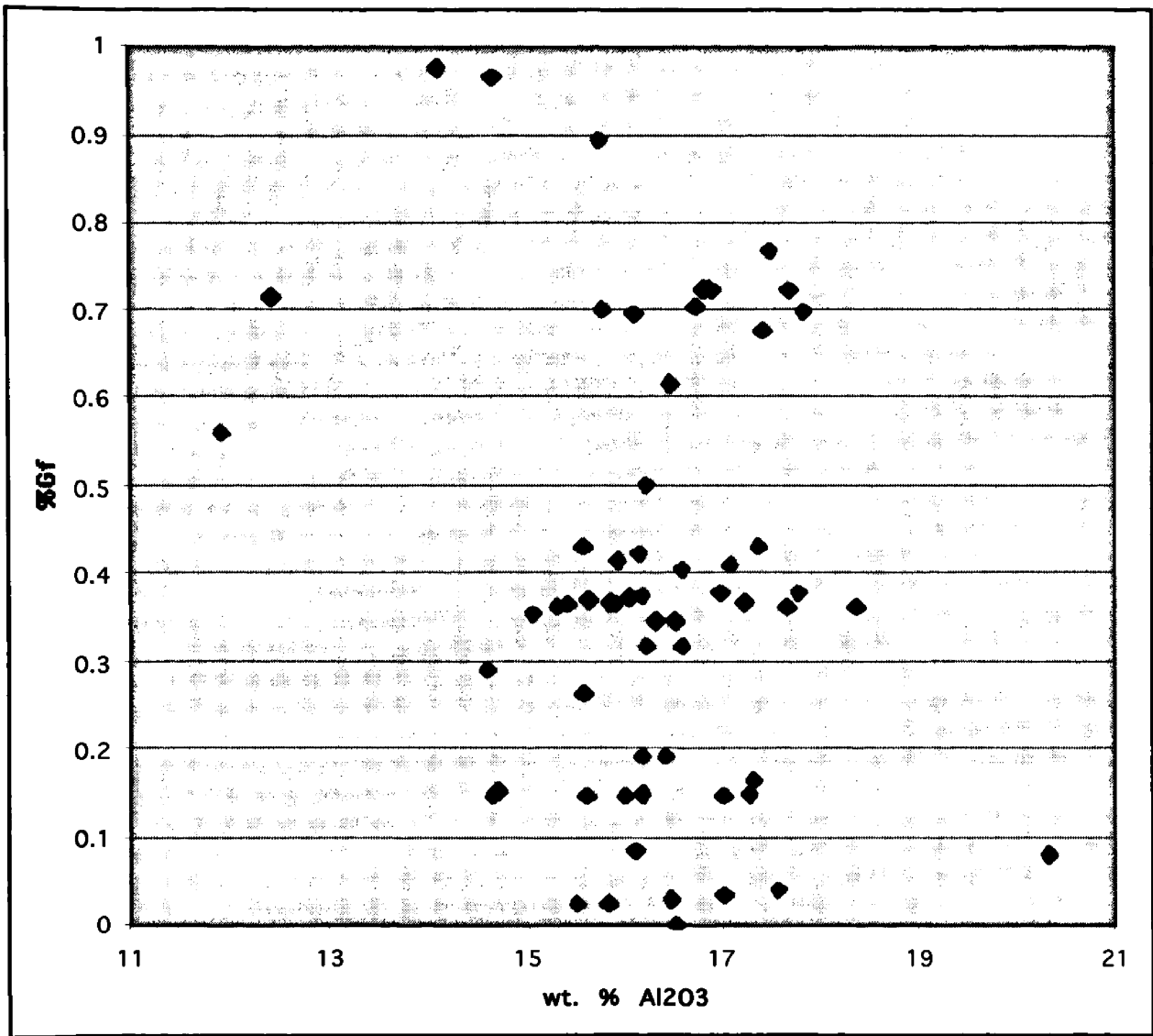


Figure 25. Plot of %Gf vs. wt. % Al₂O₃ for zero order samples.

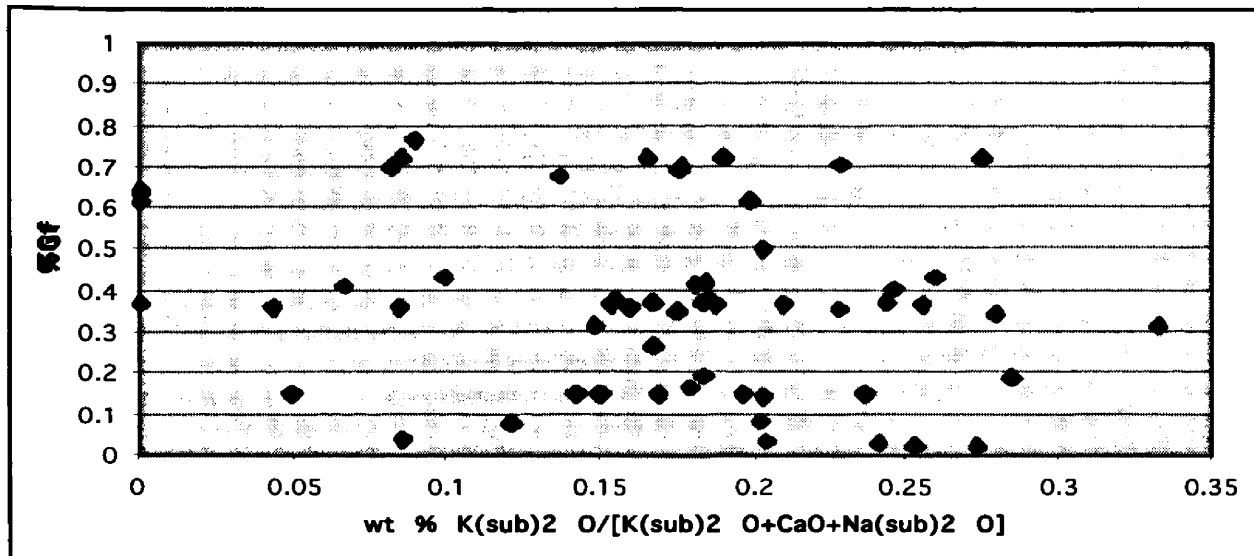


Figure 26a. Plot of %Gf vs. wt. % K₂O/(K₂O + CaO + Na₂O) for zero order samples.

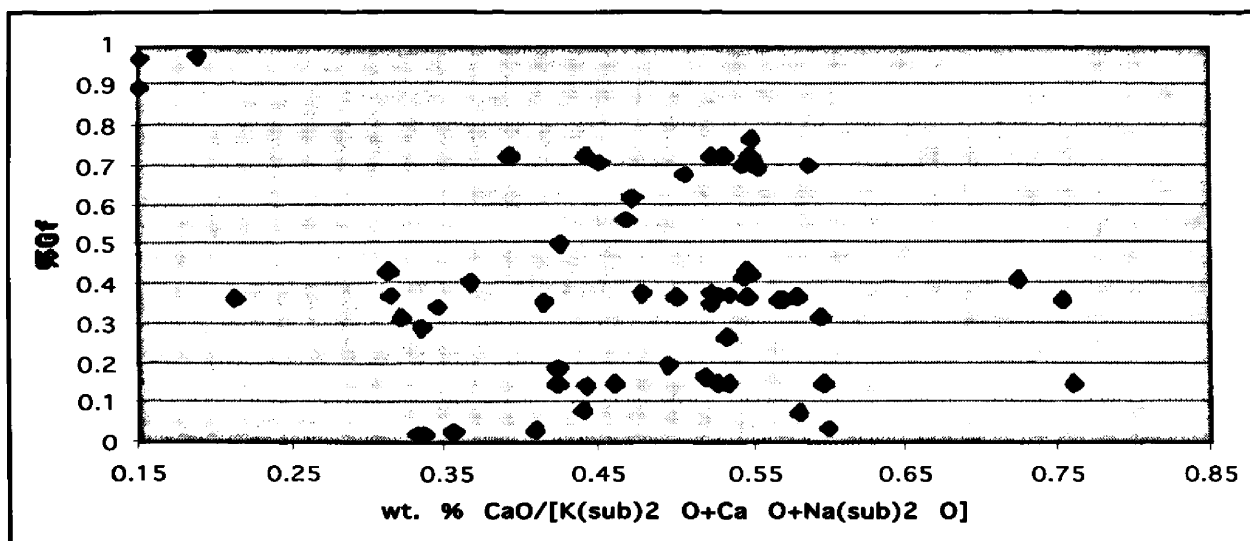


Figure 26b. Plot of %Gf vs. wt. % CaO/(K₂O + CaO + Na₂O) for zero order samples.

order samples. These %Gf numbers are plotted versus SiO₂, and Figures 25 through 26 shows the %Gf data plotted vs. Al₂O₃, K₂O/(K₂O + CaO + Na₂O), and CaO/(K₂O + CaO + Na₂O) for the zero order data. The horizontal trends are artificial manifestations of the process, and correspond to the average values of each of the lithic fragment types. Any deviation from these average values of glass used for each lithic fragment is a result of true mixing between lithic fragment types/textures in the host lava.

DISCUSSION

Zero Order Data

Initial inspection of the plotted data suggest that only general characterizations of ‘rhyolite’, ‘andesite’, and ‘basalt’ source can be used in this system, and even these should be used with mineralogic or other supporting evidence. As shown in the data, volcanic rock textures are too unconstrained to be used by this type of system. Two illustrations of this can be seen on any of the Figures 18 - 21. Not only do specific compositions of SiO₂ content have a wide variety of lithic ratios, but a wide variety of compositions can be found at a specific lithic ratio. If the system were more ideal, then all of the graphs in Figures 18 - 21 would show well defined relationships that could be used to predict lithic ratios from a specific composition. It is true that there are distinct clusters of high values at their predicted places. For example, most of the extreme data for high L_{vm}/L_{vT} ratios (Figure 20b) are found in the window of 56 - 65 wt. % SiO₂. However, there is also a cluster of data without high L_{vm}/L_{vT} ratios in that window, and even some samples in that window without any L_{vm} component. This leads to the conclusion that the data are far too erratic to use in a manner that could determine the composition from a suite of volcanic lithic fragments. One possible exception is in the

case of a rock rich in microlitic material (possible future lithic fragment) which can, with some qualitative confidence, be assigned to a composition of 56 - 65 wt. % SiO₂. Such an assumption has no valid statistical or quantitative basis. Plots of other normalized lithic types vs. SiO₂ are even more unpredictable (e.g. lathwork (54 - 66 wt. % SiO₂, Figure 21), seriate (51 - 67 wt. % SiO₂, Figure 19a), and submicrolitic (55 - 64 wt. % SiO₂, Figure 20a)). This lack of statistically valid correlation on all levels can only lead to the deduction that volcanic lithic type can not be relied upon to accurately determine the parent volcanic rock composition, and can be used only in a general sense.

I hypothesize that more intermediate composition volcanic rocks would have a much lower glass content, with the extreme composition rocks, both mafic and felsic, having much higher glass content, on average. This is far from the case, with the intermediate compositions (55 - 70 wt. %SiO₂) having a wide range of %Gf (Figure 22). With limited data, it does appear that the most felsic rocks (>70 wt. % SiO₂) produced high %Gf (greater than 65%) and very mafic rocks (<55 wt. % SiO₂) produced medium to high %Gf (25 - 60 %). It is possible, however, that these results relate partially from a sample bias toward intermediate volcanic rocks in this study (Figure 27).

Obviously, oversimplifications have produced the erratic behavior in the data from the use of these simple volcanic lithic fragments. There are too many confounding variables that produce too wide of a range of volcanic textures to relate back to specific compositions. These variables may include, but are not limited to: eruptive setting (e.g. subaqueous vs. subarial eruptions), volatile contents, alkalinity, and eruption style (pyroclastic vs. flow). All of these factors are very important for magma dynamics, but are nearly impossible to identify in a sand-sized particle, mainly due to the high alteration and degradation potential of detrital volcanic grains.

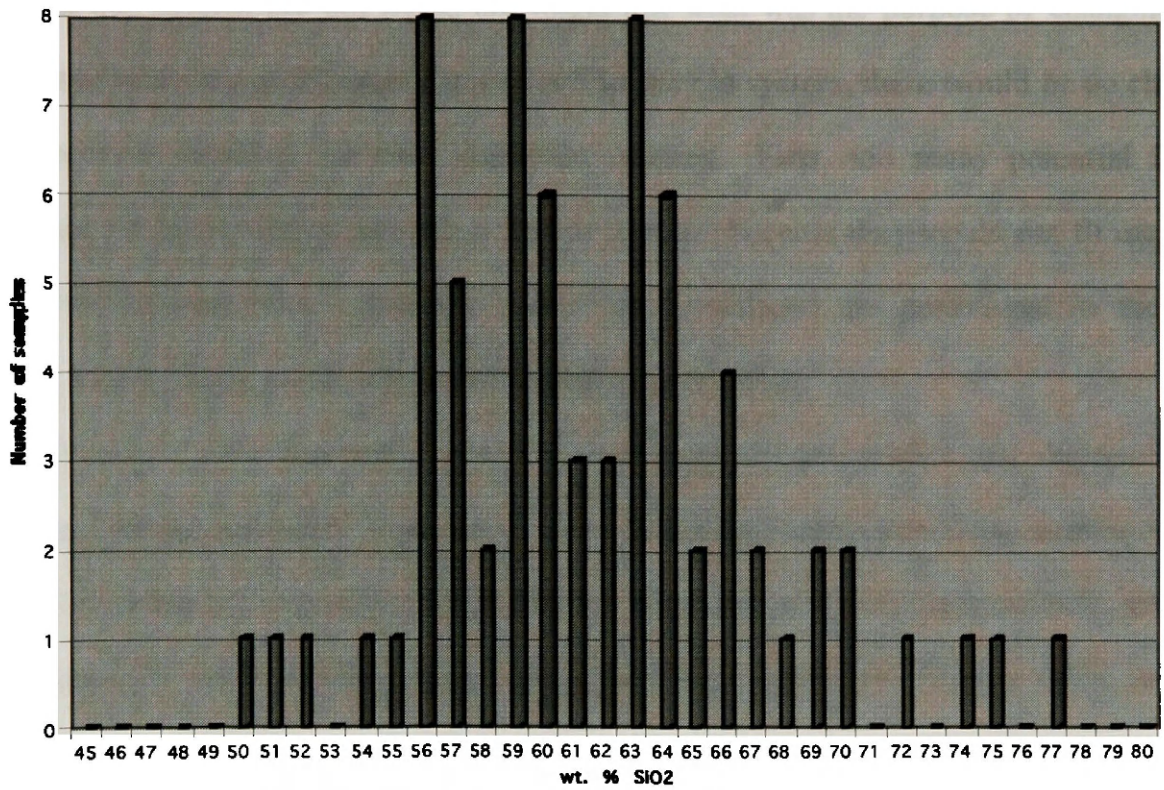


Figure 27. Histogram of sample suite, based upon wt. % SiO₂ on x-axis. Note the concentration of intermediate samples.

If this system did not work, one might ask what was the purpose of changing the methods of selecting point count categories? In the old system, there would be no chance of the system working, for two important reasons. First, too many potential lithic fragments would be labeled as unidentified or 'seriate' because they would not fit into the predetermined categories. Secondly, since the boundaries are gradational in the old system, counts likely would not be statistically quantifiable.

Volcanic lithic fragments can still be used in provenance studies (e.g., Ingersoll and Cavazza, 1991), especially when some information is known about the source rocks. Ternary diagrams of volcanic lithic fragment types used to differentiate tectonic settings (e.g. Marsaglia and Ingersoll (1992); Marsaglia (1993); Marsaglia (2004)), could still be utilized with confidence. Plots of L_{vf} - L_{vm} - L_{vl} (where $L_{vf} = L_{vg} + L_{vs}$) have been demonstrated to distinguish not only different tectonic systems, but domains and elements within tectonic systems (e.g. forarc and backarc basins, Marsaglia (1992)). Volcanic lithic fragments are still some of the most diagnostic sedimentary particles and should still be used for tectonic inference and presence of volcanism.

First Order Data

The established theory for volcanic lithic degradation is that volcanic glass is one of the most unstable sedimentary particles. Therefore, downstream trends should show a selective degradation of the more glass rich lithic fragments, relative to the more crystal rich lithic fragments. As is clear from Figures 23 and 24, neither the Owens River Gorge (Bishop Tuff) sands nor the Red Hill (Coso Volcanics) sands collected in this project showed a qualitative or statistically valid trend of declining percent glass downstream (Table 5). This lack of a trend could have two possible explanations. First, these sites

Table 5

Analysis of first order data (Bishop Tuff sands)

In order to show if there is an effect of downstream transport in the Bishop Tuff area (Figure 23), I performed a two factor analysis of variance (ANOVA), as shown in Zar (1999, Section 12.3, pg. 249-250). Since there are no replications, a special ANOVA must be performed, in which the total sums of squares (SS_{total}) is equal to the cell sums of squares (SS_{cell}). By definition, the error sums of squares (SS error) is assumed to represent error without interaction. The first factor, A, would be the three (a=3) size fractions of the sediment. The second factor, B, would be the four (b=4) sampling localities. An underlying assumption that interaction between A and B is not important. Below is the two-way ANOVA table used in this analysis. The initial hypotheses used in this analysis were:

Ho1: There is no effect of grain size on %Gf.

Ho2: There is no effect of transport on %Gf.

Source of Variation	Sums of squares (SS)	Degrees of Freedom	Mean Square	F-test	Significance
Factor A (distance)	.04942	3	.013	3.766	.00000
Factor B (grain size)	.01722	2	6.586	1.968	.22025
Intercept*	6.58601	1	.009	1505.373	.07845
Error	.02625	6	.016	-	-
Total	6.67890	12	.004	-	-

*The intercept factor (scaling factor) is for the true total mean of the data, and it's low significance indicates an F-test for Ho: $\mu=0$.

Table 5 (cont.)

The result of .07845 for the significance of downstream distance as a factor is not a statistically significant result. Transformed data (percentage data is often transformed by a square root/arc sine transformation for small and large percentages to maintain normality) showed a similar result of .09047. The proximity to the .05 professionally accepted cutoff is a signal that with further stream transport, a statistically significant trend in the degradation of the glass in the lithic population is likely. Therefore, Ho1 is cautiously accepted, and Ho2 is easily accepted.

A similar analysis was performed for the Coso data (Figure 24) with no significant or near significant results.

were chosen because of access and because they would best approximate a single source. However, the length of transport in both systems (~1 mile at Red Hill and ~4 miles at the Owens River Gorge) was most likely not enough transport to significantly change the lithic character. The second possibility is that there is no relative degradation between the volcanic lithic fragments, and the amount of glass in each lithic has no effect on the rate at which that lithic category degrades. To verify this, a much longer transport distance must be used.

Another interesting observation from Figures 23 and 24 is the lack of consistency between the size fractions. Since volcanic glass is chemically unstable, it would be easy to assume that surface area to volume ratio was the governing factor on the weathering potential of volcanic lithic fragments. For example, it might be assumed that the fine fractions have a higher surface area/volume ratio and therefore should have the lowest %Gf. However, Figures 23 and 24 show no trends across size fractions. Again, there are two possibilities for this result. First, the relative %Gf fluctuations from site to site could be due to natural randomness involved with sampling a larger somewhat heterogeneous population that one might expect in a river system. Second, the lack of trend could be a factor of the limitations in transport distance, which could obscure the true interdependence. It seems that the transport distance would not be a factor in the presence of a correlation between grain size and percent glass. Factors such as climate or acidity would appear more important to the relationship.

Volcanic lithic fragments have long been used for inferring tectonic history and provenance. However, the system by which volcanic lithic fragments are identified is fundamentally flawed, and would be better suited if the lithic fragments were defined based upon the proportions of glass, anhedral, subhedral, and euhedral microlites in the matrix.

Even with a more rigorous and scientific definition of microtextures, volcanic lithic fragments still can not be used to accurately identify the composition of the parent volcanic rock. I have shown this to be true not only for each type of lithic fragment, but also by the approximate glass content of the total lithic fragments produced by a system. While the data set was limited, it was sufficient to show the variation in volcanic rock texture that could result. The data also showed that a wide range of lithic fragment types can result from a specific composition, and a correspondingly wide range of compositions that can lead to a specific lithic fragment type. The relationships shown in the data are very complex, and require future study.

The relative degradation of the lithic types is unknown, but is assumed to depend on the amount of glass in each lithic type. Data attempting to confirm or deny this idea using first order stream samples was inconclusive. There was also shown to be no valid trend between different size fractions and their relative glass contents.

REFERENCES*

Anderson, A. T., Davis, A. M., and Lu, F., 2000, Evolution of the Bishop Tuff rhyolitic magma based on melt and magnetite inclusions and zoned phenocrysts; *Journal of Petrology*, v. 41, n. 3, p. 449-473.

Bacon, C. R. and Metz, J., 1984, Magmatic inclusions in rhyolites, contaminated basalts, and compositional zonation beneath the Coso volcanic field, California; *Contribution to Mineralogy and Petrology*, v. 85, n. 4, p. 346-365.

Carroll, A. R., Graham, S. A., Hendrix, M. S., Ying, D., Zhou, D., 1995, Late Paleozoic tectonic amalgamation of northwestern China: Sedimentary record of the northern Tarim, northwestern Turpan, and southern Juggar Basins; *GSA Bulletin*, v. 107, n. 5, p. 571-594.

Christiansen, R. L., 2001, *Geology of Yellowstone National Park: The Quaternary and Pliocene Yellowstone Plateau volcanic field of Wyoming, Idaho, and Montana*; USGS Professional Paper 729-G, 145 p.

Critelli, S. and Ingersoll, R. V., 1995, Interpretation of neovolcanic versus paleovolcanic sand grains: an example from Miocene deep-marine sandstone of the Topanga Group (Southern California); *Sedimentology*, v. 42, p. 783-804.

Davidson, J. P. and Harmon, R. S., 1989, Oxygen isotope constraints on the petrogenesis of volcanic arc magmas from Martinique, Lesser Antilles; *Earth and Planetary Science Letters*, v. 95, n. 3-4, p. 255-270.

Dickinson, W. R., 1970, Interpreting detrital modes of graywacke and arkose; *Journal of Sedimentary Petrology*, v. 40, n. 2, p. 695-707.

Dickinson, W. R., 1985, Interpreting provenance relations from detrital modes of sandstones. *In* Zuffa, G. G. (ed.), *Provenance of Arenites*, NATO Advanced Study Series, v. 148, D. Reidel Publishing Company, p. 333-361.

Dickinson, W. R. and Suczek, C. A., 1979, Plate tectonics and sandstone compositions; *American Association of Petroleum Geologists Bulletin*, v. 63, p. 2164-2182.

Gazzi, P., 1966, Le arenarie del flysch sopracretaceo dell'Appennino modenese: correlazioni con il flysch di Monghidoro; *Mineralogica e Petrographica Acta*, v. 12, p. 69-97.

Graham, S. A., Ingersoll, R. V., Dickinson, W. R., 1976, Common provenance for lithic

grains in carboniferous sandstones from Ouachita Mountains and Black Warrior Basin; *Journal of Sedimentary Petrology*, v. 46, n. 3, p. 620-632.

Hildreth, E. W., 1977, The magma chamber of the Bishop Tuff: gradients in temperature, pressure, and composition; Doctoral Thesis, University of California, Berkeley, 328 p.

Hobden, B. J., 1997, Modeling magmatic trends in time and space: eruptive and magmatic history of Tongariro volcanic complex, New Zealand; Ph. D. Thesis, Christchurch, University of Canterbury.

Holloway, C. D., Petrology of the Eocene volcanic sequence, Nez Perce and Blue Joint Creeks, southern Bitterroot Mountains, Montana; M. S. Thesis, University of Montana, Missoula, MT, 129 p.

Horton, B. K., Hampton, B. A., LaReau, B. N., and Baldellón, E., 2002, Tertiary provenance history of the northern and central Altiplano (Central Andes, Bolivia): A detrital record of plateau-margin tectonics; *Journal of Sedimentary Research*, v. 72, n. 5, p. 711-726

Ingersoll, R. V., 1990, Actualistic sandstone petrofacies: Discriminating modern and ancient source rocks; *Geology*, v. 18, p. 733-736.

Ingersoll, R. V., Bullard, T. F., Ford, R. L., Grimm, J.P., Pickle, J. D., and Sares, S. W., 1984, The effect of grain size on detrital modes: a test of the Gazzi-Dickinson point-counting method; *Journal of Sedimentary Petrology*, v. 54, p. 103-116.

Ingersoll, R. V., and Cavazza, W., 1991, Reconstruction of Oligo-Miocene volcanoclastic dispersal patterns in north-central New Mexico using sandstone petrofacies; *SEPM Special Publication 45*, p. 227-236.

Ingersoll, R. V., Kretchmer, A. G., and Valles, P. K., 1993, The effect of sampling scale on actualistic sandstone petrofacies; *Sedimentology*, v. 40, p. 937-953.

LaPoint, D. D., 1977, Geology of a portion of the Eocene Sylvan Pass volcanic center, Absaroka Volcanic Range, Wyoming; M. S. Thesis, University of Montana, Missoula, MT.

Large, E. and Ingersoll, R. V., 1997, Miocene and Pliocene sandstone petrofacies of the northern Albuquerque Basin, New Mexico, and implications for evolution of the Rio Grande Rift; *JSR*, v. 67, n. 3, 1997, p. 462-468.

Leppert, D. E., 1985, Differentiation of a shoshonitic magma at Snake Butte, Blaine

County, Montana; M. S. Thesis, University of Montana, Missoula, MT.

Lindsay, C. R., 2002, Petrogenesis of Eocene calc-alkaline magmatism at Electric Peak and Sepulcher Mountain, Absaroka Volcanic Province, Montana and Wyoming; M. S. Thesis, Montana State University, Bozeman, MT.

Lindsay, C. R., and Feeley, T. C., 2003, Magmagenesis at the Eocene Electric Peak-Sepulcher Mountain complex, Absaroka Volcanic Province, USA; *Lithos*, v. 67, p. 53-76.

Lundberg, N., 1991, Detrital record of the early Central American magmatic arc: Petrography of intraoceanic forarc sandstones, Nicoya Peninsula, Costa Rica; *GSA Bulletin*, v. 103, n. 7, p. 905-915.

Luthy, S. T., 1981, Petrology of Cretaceous and Tertiary intrusive rocks, Red Mountain - Bull Trout Point area, Boise, Valley, and Custer counties, Idaho; M. S. Thesis, University of Montana, Missoula, MT.

Marsaglia, K. M., 1992, Petrography and provenance of volcanoclastic sands recovered from the Izu-Bonin arc. In Taylor, B., et al., *Proceedings of the Ocean Drilling Program, Scientific Results*, v. 126, p. 139-154.

Marsaglia, K. M., 1993, Basaltic island sand provenance. In Johnson, M. J., and Basu, A. (eds.), *Processes Controlling the Composition of Clastic Sediments*; GSA Special Paper 284, Boulder, Colorado, p. 41-65.

Marsaglia, K. M., 2004, Sandstone detrital modes support Magdalena Fan displacement from the mouth of the Gulf of California; *Geology*, v. 32, n. 1, p. 45-48.

Marsaglia, K. M., and Ingersoll, R. V., 1992, Compositional trends in arc-related, deep-marine sand and sandstone: A reassessment of magmatic-arc provenance; *GSA Bulletin*, v. 104, p. 1637-1649.

Nesse, W. D., 1991, *Introduction to optical mineralogy*, 2nd edition; Oxford University Press, New York, 335 p.

Novak, S. W. and Bacon, C. R., 1986, Pliocene volcanic rocks of the Coso Range, Inyo County, California; USGS Professional Paper 1383, 44 p.

Schmicke, H.-U., 1981, Ash from vitric muds in deep sea cores from the Mariana Trough and fore-arc region (South Philippine Sea) (Sites 453, 454, 455, 458, 459, and SP), Deep Sea Drilling Project Leg 60. In Hussong, D. M., Uyeda, S., et al., *Initial Reports of the Deep Sea Drilling Project, 60*; Washington (U. S. Government Printing Office), p. 473-

481.

Suttner, L. J., 1974, Sedimentary petrographic provinces: An evaluation; SEPM Special Publication 21, p. 75-84.

Van Der Plas, L. and Tobi, A. C., 1965, A chart for judging the reliability of point counting results; American Journal of Science, v. 263, p. 87-90.

Williams, H., Turner, F. J., and Gilbert, C. M., 1954, Petrography: An introduction to the study of rocks in thin sections; W. H. Freeman and Co., San Fransisco, 406 pp.

Zar, J. H., 1999, Biostatistical analysis, fourth edition; Prentice Hall, Upper Saddle River, New Jersey, 663 pp.

Zuffa, G. G., 1985, Optical analysis of arenites: influence of methodology on compositional results. *In* Zuffa, G. G. (ed.), Provenance of Arenites, NATO Advanced Study Series, v. 148, D. Reidel Publishing Company, pg. 165-189.

***Note:** Sample references may not be directly in text. Some samples are from unpublished or widely published work, and a reference for a specific sample may only be representative.

Appendix I - Complete Point Count Data Set

Date, Sample #	%SiO2	Reference	Qm	P	K	M	Dpao	Dox	O	U
7-16, Tr 191	76.93	Luthy 81	18	10	7	5	1	2		
7-17, 39C	49.6	Leppert 85		30			49			5
?, 32L	51.68	Leppert 85					1		27	
7-21, 260A	69.2	Holloway 80	37	37	73	5	1			1
?, 70A	74.8	Holloway 80	6	2	3	3				
?, 54A	73.22	Holloway 80	39	43	47	8				
7-24?, 66A ttf	71.0	Holloway 80	4	1						
7-27, EPR 334	54.0	LaPoint 77		89		5	53	4		1
?, EPR 233	63.2	LaPoint 77		127	2	19	2	1		
9-10, SM9701	62.78	Lindsay 03		105			24	4		
9-11, SM9702	63.56	Lindsay 03		92			17	2		
9-12, SM9713	62.16	Lindsay 03		113			24	2		
?, SM9733	65.42	Lindsay 03		146		4	19	1		
9-26, SM9726	58.50	Lindsay 03		44		2	34			1
9-13, SM9828	55.81	Lindsay 03		42			34			
9-13, SM9703	63.71	Lindsay 03		115			7	4		3
9-13, SM9738	62.54	Lindsay 03		48			34	1		
9-13, SM9730	66.57	Lindsay 03		104		8	26			
?, SM9704	62.58	Lindsay 03		24			42			
?, SM9712	56.27	Lindsay 03		52			31			
?, SM9734	67.07	Lindsay 03	1	144		8	30	2		
9-17, SM9737	57.40	Lindsay 03		17			30			
9-21, SM9827	57.79	Lindsay 03		66			41			
9-18, SM9719	62.60	Lindsay 03		100			13	1		
9-21, SM9732	65.70	Lindsay 03		117		11	6			
9-21, SM9705	62.09	Lindsay 03		45			27	5		1

Appendix I - Complete Point Count Data Set (continued)

Date, Sample #	LvT	Lvv	Lvg	Lvs	Lva	Lvsm	Lvm	Lvl	%Gf	Total Points
7-16, Tr 191	457	313	37	104	3				.675	500
7-17, 39C	416	1	2	3	8		172	230	.559	500
?, 32L	472			239	4		101	128	.290	500
7-21, 260A	346			17	329				.453	500
?, 70A	486	486							.975	500
?, 54A	363	359		3	1				.964	500
7-24?, 66A ttf	495	413	80	2					.894	500
7-27, EPR 334	345			1	5		35	304	.677	500
?, EPR 233	341		6	335					.033	492
9-10, SM9701	367				4		13	350	.705	500
9-11, SM9702	389			9	9	371			.501	500
9-12, SM9713	361						2	359	.723	500
?, SM9733	330			326			4		.029	500
9-26, SM9726	419			1	2		21	395	.702	500
9-13, SM9828	424			25	2	385	12		.148	500
9-13, SM9703	371			225	8	118	19	1	.084	500
9-13, SM9738	417							417	.725	500
9-13, SM9730	362			358	4				.025	500
?, SM9704	434			2	6	426			.147	500
?, SM9712	417			2	9	92	312	2	.317	500
?, SM9734	315			315					.025	500
9-17, SM9737	453						453		.375	500
9-21, SM9827	393			1	11		381		.364	500
9-18, SM9719	386			5	7	374			.146	500
9-21, SM9732	366			30			336		.346	500
9-21, SM9705	422			4	3	415			.148	500

Appendix I - Complete Point Count Data Set (continued)

Date, Sample #	%SiO2	Reference	Qm	P	K	M	Dpao	Dox	O	U
9-22, SM9727	59.02	Lindsay 03		30			27	1		
9-22, SM9724	68.43	Lindsay 03		100			17			
9-24, SM9810	64.43	Lindsay 03		35			27			
9-23, SM9721	58.38	Lindsay 03		67			43			2
9-25, SM9723	59.05	Lindsay 03		57			30			
2-24, SM9716	58.80	Lindsay 03		56			55			
9-26, SM9720	58.42	Lindsay 03		62			41			1
9-25, SM9731	64.29	Lindsay 03		117						
9-26, SM9725	61.34	Lindsay 03		108						
9-27, SM9740	63.84	Lindsay 03		130						
9-27, SM9715	61.05	Lindsay 03		75						
9-28, SM9718	58.6	Lindsay 03		92						
9-27, SM9706	69.35	Lindsay 03		144						
10-4, SM9736	59.07	Lindsay 03		5						
10-1, SM9709	58.01	Lindsay 03		83						
10-4, SM9735	68.95	Lindsay 03		130		4	11	2		
10-4, TLC9701	63.83	Lindsay 03		54		6	37	2		
10-7, SM9722	60.36	Lindsay 03		124						
10-7, SM9826	58.75	Lindsay 03		64			40			
10-8, SM9717	59.51	Lindsay 03		89			1			
12-15, TG001	55.44	Hobden 97		128			51			4
12-16, TG004	55.06	Hobden 97		141			49			1
12-17, TG010	56.93	Hobden 97		97			39	2		2
12-17, TG575	55.06	Hobden 97		113			68			
12-18, TG041	55.19	Hobden 97		128			48			
12-17, TG019	56.51	Hobden 97		108			35			

Appendix I - Complete Point Count Data Set (continued)

Date, Sample #	LvT	Lvv	Lvg	Lvs	Lva	Lvsm	Lvm	Lvl	%Gf	Total Points
9-22, SM9727	442			2	10	429		1	.147	500
9-22, SM9724	383			1			382		.374	500
9-24, SM9810	438			26			412		.354	500
9-23, SM9721	388				12		318	58	.416	500
9-25, SM9723	413			1	8	6	364	4	.367	500
2-24, SM9716	389			3	1	184	201		.265	500
9-26, SM9720	396			4	7		11	374	.695	500
9-25, SM9731	370			13		73	284		.318	500
9-26, SM9725	380				1	2	114	263	.615	500
9-27, SM9740	343				1		310	32	.407	500
9-27, SM9715	386			1	3	12	368	2	.366	497
9-28, SM9718	351			1	18	6	254	72	.423	499
9-27, SM9706	325		232	89	3		1		.362	499
10-4, SM9736	477				2	56	418	1	.348	500
10-1, SM9709	393			29	10	306	48	48	.164	500
10-4, SM9735	353		303	50					.433	500
10-4, TLC9701	401					328	73		.191	500
10-7, SM9722	348			7	14	250	76	1	.192	500
10-7, SM9826	396			1	8		383	4	.370	500
10-8, SM9717	409					9	390	10	.379	500
12-15, TG001	316			2		2	64	248	.646	500
12-16, TG004	307		1						.619	500
12-17, TG010	360		10	8	1	5	329	7	.373	500
12-17, TG575	319	1				8	67	243	.638	500
12-18, TG041	324				1		10	313	.712	500
12-17, TG019	357		3		1			353	.721	500

Appendix I - Complete Point Count Data Set (continued)

Date, Sample #	%SiO2	Reference	Qm	P	K	M	Dpao	Dox	O	U
12-19, TG043	56.51	Hobden 97		112			38			2
12-18, TG540	56.71	Hobden 97		81			18			
12-20, P39864	55.82	Hobden 97		77			30			1
12-20, P39850	55.71	Hobden 97		128			37			
1-10, SL8321	65.98	Davidson 89	41	86	53	15	24			
1-11, M8217	58.94	Davidson 89		138	10		5	1		
1-13, M8225	60.26	Davidson 89		133			25	9		
1-12, SL8326	53.47	Davidson 89		180			60			1
1-14, SL8308	66.23	Davidson 89	35	152	30	1	23	1		
1-13, SL8324	65.49	Davidson 89	12	156	50	1	21	10		
1-14, M8328	55.00	Davidson 89		66			92	3		2
1-14, M8277	60.47	Davidson 89		63	4		14	5		
1-15, M8222	59.14	Davidson 89		197	1		48	8		
1-15, M8228	62.10	Davidson 89	47	119	73	2	31			1
1-19, SL8316	63.76	Davidson 89	30	50	120	1	26	5		
1-20, M8268	62.86	Davidson 89	16	86	86		43	8		
1-19, M8214	61.10	Davidson 89		106	56		28	13		
1-20, M8310	50.03	Davidson 89		149	1		38	2		
1-20, M8270	59.39	Davidson 89		140	26			1		

Appendix I - Complete Point Count Data Set (continued)

Date, Sample #	LvT	Lvv	Lvg	Lvs	Lva	Lvsm	Lvm	Lvl	%Gf	Total Points
12-19, TG043	348			1		337	9	1	.157	500
12-18, TG540	401	10	25		6		11	349	.697	500
12-20, P39864	392	2	2	1	1			386	.721	500
12-20, P39850	335	1		3	1	1	7	322	.708	500
1-10, SL8321	281	7		1	1	1		271	.724	500
1-11, M8217	346		1	309		36			.039	500
1-13, M8225	333				1		1	331	.722	500
1-12, SL8326	259						15	244	.362	500
1-14, SL8308	258	1					3	254	.722	500
1-13, SL8324	250		186	63	1				.378	500
1-14, M8328	337			2	6	324	3	2	.152	500
1-14, M8277	414	71						343	.768	500
1-15, M8222	246	3				4	14	225	.699	500
1-15, M8228	227		194	33					.431	500
1-19, SL8316	265			1		8	256		.367	497
1-20, M8268	261				1	260			.149	500
1-19, M8214	297					18	278	1	.363	500
1-20, M8310	310			1	3	5	262	39	.411	500
1-20, M8270	333			189		143	1		.080	500

Appendix I - Complete Point Count Data Set (cont., First Order Data)

Date, Sample #	%SiO ₂	Reference	Qm	P	K	M	Dpao	Dox	O	U
10-23, COS1A-c	51.7-54.0	Bacon Metz 84		41			10			
2-21, COS1A-m	51.7-54.0	Bacon Metz 84		91	1		49	1		1
2-16, COS1A-f	51.7-54.0	Bacon Metz 84		40	1		19			2
11-12, COS1B-c	51.7-54.0	Bacon Metz 84		15			4			
2-23, COS1B-m	51.7-54.0	Bacon Metz 84		47	3		32	3	7	12
10-23, COS1B-f	51.7-54.0	Bacon Metz 84	1	42	1	1	10			2
11-14, COS1C-c	51.7-54.0	Bacon Metz 84	71	54	147		8	1	29	
2-21, COS1C-m	51.7-54.0	Bacon Metz 84	85	82	166	1	6	1	15	8
2-15, COS1C-f	51.7-54.0	Bacon Metz 84	97	144	68	8	17	1	9	9
10-2, BT1A-c	75.5-77.6	Hildreth 77	24	4	24				20	
2-14, BT1A-m	75.5-77.6	Hildreth 77	59	41	99	1	2	3	23	3
2-18, BT1A-f	75.5-77.6	Hildreth 77	117	42	65		14	3	6	2
2-21, BT1B-c	75.5-77.6	Hildreth 77	19	5	24		4	1	6	9
2-24, BT1B-m	75.5-77.6	Hildreth 77	91	27	48	3	1	1	8	
2-23, BT1B-f	75.5-77.6	Hildreth 77	78	33	66	6	4		5	5
11-14, BT1C-c	75.5-77.6	Hildreth 77	2	2	4			3	1	1
2-14, BT1C-m	75.5-77.6	Hildreth 77	15	6	17	1		2	4	1
11-13, BT1C-f	75.5-77.6	Hildreth 77	87	10	47	2	3	1	1	1
2-20, BT1D-c	75.5-77.6	Hildreth 77	11	4	30			2	1	
10-25, BT1D-m	75.5-77.6	Hildreth 77	135	46	70				10	2
2-26, BT1D-f	75.5-77.6	Hildreth 77	66	31	43	3	5	2	5	
3-25, COS1A-m(1)	51.7-54.0	Bacon Metz 84		95			86			
3-25, COS1A-m(2)	51.7-54.0	Bacon Metz 84	2	116			60			2
3-25, COS1A-m(3)	51.7-54.0	Bacon Metz 84	2	122	1		87	1		
3-25, COS1A-m(4)	51.7-54.0	Bacon Metz 84	3	91			83	1		1

Appendix I - Complete Point Count Data Set (cont., First Order Data)

Date, Sample #	LvT	Lvv	Lvg	Lvs	Lva	Lvsm	Lvm	Lvl	%Gf	Total Points
10-23, COS1A-c	349					113	73	163	.466	400
2-21, COS1A-m	257	27				25	68	137	.639	400
2-16, COS1A-f	338	91		1	1	2	22	221	.762	400
11-12, COS1B-c	381	6		21		102	152	100	.397	400
2-23, COS1B-m	296	64		5		38	67	122	.614	400
10-23, COS1B-f	346	18	1			132	43	152	.474	403
11-14, COS1C-c	90	23		2		5	13	47	.691	400
2-21, COS1C-m	36	10	1			4	9	12	.637	400
2-15, COS1C-f	47	11	1	3		7	3	22	.626	400
10-2, BT1A-c	328	244	57	9	1		1	16	.849	400
2-14, BT1A-m	169	59	1	8		27	16	58	.653	400
2-18, BT1A-f	151	77	15	6		5	8	40	.765	400
2-21, BT1B-c	332	96	79	1		9	21	126	.704	400
2-24, BT1B-m	221	116	29	9		2	15	50	.769	400
2-23, BT1B-f	203	87	14	11		9	15	66	.724	400
11-14, BT1C-c	387	333	7				6	41	.931	400
2-14, BT1C-m	354	160	35	9	1	20	24	105	.740	400
11-13, BT1C-f	248	194	1	24		7	2	11	.845	400
2-20, BT1D-c	352	80	88	4		13	38	129	.659	400
10-25, BT1D-m	137	77	9	36		11	4		.610	400
2-26, BT1D-f	245	97	14	23		13	21	77	.685	400
3-25, COS1A-m(1)	319	33				37	86	163	.590	500
3-25, COS1A-m(2)	320	22		3		46	70	179	.576	500
3-25, COS1A-m(3)	287	15		2		30	68	172	.590	500
3-25, COS1A-m(4)	321	14		1		42	91	173	.560	500